AWARD NUMBER: **W81XWH-13-1-0139**

TITLE: Targeting Common but Complex Proteoglycans on Breast Cancer Cells and Stem Cells Using Evolutionary Refined Malaria Proteins

PRINCIPAL INVESTIGATOR: **Ali Salanti**

CONTRACTING ORGANIZATION: **University of Copenhagen**
Nørregade 10, 1165 K, Denmark

REPORT DATE: **November 2015**

TYPE OF REPORT: **Final Report**

PREPARED FOR: U.S. Army Medical Research and Materiel Command
Fort Detrick, Maryland 21702-5012

REPORT DOCUMENTATION PAGE

Form Approved
OMB No. 0704-0188

1. REPORT DATE	2. REPORT TYPE	3. DATES COVERED
November 2015	Final	15Aug2013 - 14Aug2015

4. TITLE AND SUBTITLE

Targeting Common but Complex Proteoglycans on Breast Cancer Cells and Stem Cells Using Evolutionary Refined Malaria Proteins

5a. CONTRACT NUMBER
W81XWH-13-1-0139

5b. GRANT NUMBER
W81XWH-13-1-0139

5c. PROGRAM ELEMENT NUMBER

6. AUTHOR(S)
Professor Ali Salanti

E-Mail: Salanti@sund.ku.dk

5d. PROJECT NUMBER

5e. TASK NUMBER

5f. WORK UNIT NUMBER

7. PERFORMING ORGANIZATION NAME(S) AND ADDRESS(ES)

University of Copenhagen.
Nørregade 10, 1165 K, Denmark

8. PERFORMING ORGANIZATION REPORT NUMBER

9. SPONSORING / MONITORING AGENCY NAME(S) AND ADDRESS(ES)

U.S. Army Medical Research and Materiel Command
Fort Detrick, Maryland 21702-5012

10. SPONSOR/MONITOR'S ACRONYM(S)

11. SPONSOR/MONITOR'S REPORT NUMBER(S)

12. DISTRIBUTION / AVAILABILITY STATEMENT

Approved for Public Release; Distribution Unlimited

13. SUPPLEMENTARY NOTES

14. ABSTRACT

We have successfully produced recombinant malaria derived VAR2CSA that binds with high affinity and high specificity to breast cancer cells and breast cancer tissue biopsies. We have demonstrated that the protein binds to distinct secondary modified proteoglycans exclusively present on breast cancer cells and that targeting these with recombinant VAR2CSA interferes with key functions of the cancer cell like growth, migration and invasion.In vivo models demonstrate that conjugation of a toxin to VAR2CSA followed by IV administration to metastatic breast cancer bearing mice completely cures the animals.

15. SUBJECT TERMS
Cancer, breast cancer, treatment, malaria protein

16. SECURITY CLASSIFICATION OF:			17. LIMITATION OF ABSTRACT	18. NUMBER OF PAGES	19a. NAME OF RESPONSIBLE PERSON
a. REPORT	b. ABSTRACT	c. THIS PAGE			USAMRMC
Unclassified	Unclassified	Unclassified	Unclassified	59	19b. TELEPHONE NUMBER *(include area code)*

Table of Contents

Page

INTRODUCTION:

In pregnant women, parasite-infected red blood cells express a protein that binds to a distinct sugar structure present only on certain cells of the placenta. This highly evolved binding system enables the parasite to evade clearance and infect placental cells, thereby causing pregnancy-associated malaria outbreaks in epidemic regions of the world. Prior to this application we discovered that human breast cancer cells express this same carbohydrate structure, which is present on human placental cells. The sugar structure likely enables breast cancer cells to migrate and invade surrounding normal tissue, and plays a role in metastatic spread of the cancer. This raised the intriguing possibility that we could use this naturally refined parasite-host interaction mechanism as a tool to specifically bind human breast cancer cells and inhibit their metastatic potential. The aim of the project was to combine our individual expertise in parasitology (Dr. Salanti) and oncology (Dr.Daugaard) to investigate the potential of exploiting the interaction between the malarial protein, called VAR2, and the breast cancer-associated sugar structure as a novel approach to inhibit growth and metastatic growth of different subtypes of breast cancers.

KEYWORDS:

Breast cancer, Malaria, treatment, metastasis, Recombinant protein, drug conjugate

ACCOMPLISHMENTS:

OVERALL PROJECT SUMMARY: We have successfully produced recombinant VAR2CSA that binds with high affinity and high specificity to breast cancer cells and breast cancer tissue biopsies. We have demonstrated that the protein binds to distinct secondary modified proteoglycans exclusively present on breast cancer cells and that targeting these with recombinant VAR2CSA interferes with key functions of the cancer cell like growth, migration and invasion. *In vivo* data supports the use of using toxin conjugated VAR2CSA to effectively target and treat breast cancer. There are no deviations to the agreed research plan and all major tasks has been finalized (see below section for breakdown of results)

Key Research Accomplishments:

Major goals and what was accomplished section:

NOTE: The below reporting relates both to work done at UBC in Dr. Daugaard's laboratories as well as the part done by Dr. Salanti in Copenhagen. Place of a given task is indicated in brackets.

RE: Major work task I (related to aim I)

A stable expression system for the production of recombinant VAR2CSA has been tested and validated in Shuffle *E. coli* cells. We can now produce sufficient amounts of recombinant protein for this project. We are currently trying to move the expression system into insect cells and are in the process of mutating glycosylation sites in the VAR2CSA protein (as glycosylation of the protein inhibits its activity). The produced proteins has been tested for binding affinity and specificity to a panel of breast cancer cells, and we have shown that both the eukaryotic and prokaryotic produced proteins binds all tested breast cancer cells with high affinity (1nM) and high specificity. Scale up batches were made and available for subsequent *in vivo* and *in vitro* experiments. The production of recombinant VAR2CSA is described in the attached published article Salanti et al, 2015. Here is also described the quality control and binding kinetics of the protein. Accordingly, the work within *major work task I* is fully accomplished. (All this work has been done at UCPH/Salanti).

RE: Major work task II (related to aim II)

To conduct the work outlined in major work task II, we tested a number of different purification technologies including the TAP-TAG approach. It turned out that the best approach was not the TAP-TAG, but a column-based approach where recombinant VAR2CSA was immobilized within a purification column. Using this approach, we have until now successfully identified a number of proteoglycans that interact with the recombinant malaria protein VAR2CSA when sulfated on carbon 4 of the CS backbone. We have identified CSPG4 as a major protein in breast cancer cells as well as CD44, expression of these has been validated using western blot. Accordingly, the work within *major work task II* is fully accomplished. (The method for pulling down breast cancer associated proteoglycans was developed at UCPH/Salanti and performed by a PhD student from UCPH working in Daugaard's laboratory)

RE: Major work task III (related to aim III)

The work described in *Subtask III-A* has been finalized. We have with success investigated the internalization patterns of recombinant VAR2CSA and found that the protein internalize into intracellular structures within 15-20 minutes after addition to the tumor cell culture and that it ends up in the lysosomal compartment. (This work has been done both at UCPH and BCCRC). These data are presented in the attached article, Salanti et al., 2015.

The work described in *Subtask III-B* is finalized. We have identified the main signalling pathway affected by recombinant VAR2CSA (Integrin signalling) and validated this biochemically and functionally. (This work is done by a PhD student enrolled at UCPH, working with Dr. Daugaard at BCCRC). Figure 1 shows that incubation of MDA-231 breast cancer cells inhibits phosphorylation of ERK and Src (panel A) and that this results in a significant decreased capacity of the breast cancer cells to migrate (panel B)

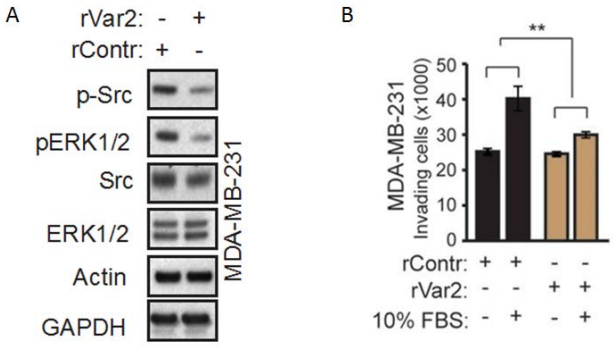

Figure 1

RE: Major work task IV (related to aim IV)

The work described in work task *IV*, has been concluded according to plan. We have successfully established an IHC procedure for high-throughput tissue analysis on the VentureDiscovery platform. An important finding here is that the fixed tissue cannot be subjected antigen retrieval procedures (otherwise used for most IHC antibodies), as this process destroys the glycosaminoglycan target on the tissue. Based on this we have identified the optimal concentration of the recombinant VAR2CSA to be 500 pM in this assay. The optimized protocol is based on a primary incubation of a V5-tagged VAR2CSA, followed by a secondary incubation with a mouse monoclonal anti-V5 antibody, finalized by a detection step using anti mouse-HRP. The data are presented in the attached article, Salanti et al.,

2015. The high throughput screening of breast cancer tissues, has been finalized with encouraging results. The data demonstrate that that we bind approximately 80-90% of the breast tumor specimens on the test array. These data are presented in the supplementary section of the attached article Salanti et al., 2015. (This work was done at VPC using protein from UCPH)

RE: Major work task V (related to aim V)

To facilitate coupling of saporin to VAR2CSA we have made a VAR2CSA protein with a biotin acceptor site and procured saporin coupled to streptavidin. We have failed to directly couple saporin to VAR2CSA without significantly reducing affinity of VAR2CSA to CSA. The biotin-VAR2 drug conjugate kills a panel of tested breast cancer cells with nM IC50 values. During the project period we developed a more clinical relevant toxin conjugation strategy in collaboration with Kairos Therapeutics. A cell cytotoxin was successfully conjugated to recombinant VAR2CSA and the drug conjugate effective kills breast cancer cells in vitro. The data are presented in the attached article Salanti et al., 2015 (This work has been done at UCPH and *in vitro* efficacy has been repeated at VPC)

RE: Major work task VI (related to aim VI)

The work outlined under Major work task VI has been finalized with minor deviations to the SOW. All subtasks were performed with the exception of the radiolabelling which we did not manage to do successfully, but we are currently working on getting this method established. Furthermore we used a xenograft metastatic mouse tumor model rather than a DMBA induced model. *In vitro* we have demonstrated that we effectively can target a range of breast cancer cells and tissue biopsies demonstrating strong proof of concept for utilizing the strategy as a preferred targeted strategy against breast cancer. We have investigating the functional consequences of VAR2CSA binding to breast cancer cells, and in vitro we have a strong effect on the adhesion phenotype. In other programs directed at other types of cancer we have evaluated the in vivo effect on tumor growth using recombinant naked VAR2CSA and the conclusion is that we have an effect on migration of cells but not on growth. For a clinical validation of the concept we would prefer to have an effect on tumor growth hence we decided to focus our efforts on the *in vivo* validation of a VAR2CSA drug conjugate. Hence we set up an efficacy model using the highly aggressive syngeneic (immunocompetent) mouse model of metastatic

murine breast cancer cells. 4T1 breast cancer cells were efficiently bound by rVAR2 in a concentration and CSA-dependent manner. Moreover, the VAR2CSA drug conjugate demonstrated strong cytotoxicity in 4T1 cells in vitro, which could be completely rescued by competition with soluble CSA. Injection of luciferase-4T1 cells in the left ventricle of the heart of C57BL/6 mice resulted in aggressive bone metastasis with an overall penetrance of 50%–60%. The bone metastases invaded into adjacent muscle and showed strong pl-CS expression as analyzed by rVAR2-based immunohistochemistry (IHC). Notably, of the mice with 4T1 bone metastases, five out of six mice in the the VAR2CSA drug conjugate -treated group were still alive at the end of the study (day 54) with no detectable metastases, while all control-treated mice died with metastatic disease ($p = 0.0196$) Indeed, the VAR2CSA drug conjugate -treatment significantly increased survival of mice with 4T1 bone metastasis as compared to control-treated mice. (This work was done at VPC using protein from UCPH). The data are presented in the attached article Salanti et al., 2015.

CONCLUSION: In summary the research was conducted and finalized according to the plan. We have managed to produce and quality control a scale up production of the malaria protein VAR2CSA. We have extensive data demonstrating that this protein specifically targets sulfated chondroitin sulfate A proteoglycans present on all tested breast cancer cells and the vast majority of tested tissue biopsies. Using pull down assays we have an overview of what the protein cores is and our functional *in vitro* assays demonstrate that targeting these proteoglycans interferes with integrin mediated focal adhesion. And most importantly our in vivo data demonstrate that VAR2CSA armed with a cellular toxin effectively can treat mice with metastatic breast cancer with no observed acute side effects or organ pathology.

Opportunity for training and professional development:

The VPC is a UBC and National Centre of Excellence, with collaborative links across on-campus and hospital-based research facilities, and is internationally recognized as a comprehensive and integrated cancer research and treatment facility. The VPC uniquely integrates many critical components of translational research under one organization, facilitating seamless management of the complex processes involved in discovery, preclinical development, commercialization, and clinical research in close partnership with national clinical trials and research networks as well as the industry. A major

strength of the VPC is the proximity of its clinical and basic research programs, oriented to direct discovery research and translate these discoveries towards the clinical arena. As part of our collaborative research project, we share several trainees that spend time both in Copenhagen and at the VPC/UBC. When trainees are at Dr. Daugaard's laboratory at the VPC they enjoy unrestricted access to 60,000 square foot integrated laboratory at the Jack Bell and Robert Ho Research Buildings as well as to core infrastructure and technology platforms to support our research project. The Daugaard lab is located in the 3rd floor in the Robert Ho Research Building and on the 5th floor of the Jack Bell Research Centre. It is comprised of a research laboratory and a molecular pathology core facility. As such, the work environment for our trainees has elements of both basic and translational cancer research and provides an optimal framework for professional development.

How were the results disseminated to communities of interest?

The first article describing this novel strategy was published in October 2015 in Cancer Cell (attached to this report). Following the publication our institutions made press releases about the publication. These press releases were well adopted by the international news medias, and Daugaard and Salanti have to date given more than 100 interviews about the research both in national as well as international medias ranging from local newspapers to national broadcasted TV.

In addition to this we have presented the results at numerous international scientific conferences.

What do you plan to do during the next reporting period to accomplish the goals?

Nothing to report.

IMPACT:

Impact on the development of the principal disciplines of the project: For the first time we demonstrate how an evolutionary evolved pathogen derived protein can be used to target malignant tissue. Furthermore we describe for the first time the presence of a uniquely cancer associated modification, which will form the basis for a multitude of novel targeting strategies.

Impact on other disciplines: The data provides novel insight into the pathology of malaria and how the malaria parasite using VAR2CSA binds to the placental receptor.

Impact on technology transfer: Nothing to report.

Impact on society beyond science and technology: The project demonstrates how basic research into malaria pathology can provide novel tools against cancer, highlighting the societal importance of basic research.

CHANGES/PROBLEMS:

Changes in approach and reasons for change: Due to time constraints caused by the shift from saporin to a more clinical relevant toxin we changed the animal model from an induced model to a xenograft model.

Actual or anticipated problems or delays and actions or plans to resolve them:

Nothing to report.

Changes that had a significant impact on expenditures:

Nothing to report.

Significant changes in use or care of human subjects, vertebrate animals, biohazards, and/or select agents:

Nothing to report.

Significant changes in use or care of human subjects:

Nothing to report.

Significant changes in use or care of vertebrate animals:

Instead of running the DMBA induced model we used a xenograft mouse model

Significant changes in use of biohazards and/or select agents

Nothing to report

PRODUCTS:

Publications, conference papers, and presentations

Key publication:
Ali Salanti, Thomas M Clausen, Mette Ø Agerbæk, Nader Al Nakouzi, Madeleine Dahlbäck2, Htoo Z Oo, Sherry Lee, Tobias Gustavsson, Jamie R Rich, Bradley J Hedberg, Yang Mao, Line Barington, Marina A Pereira, Janine LoBello, Makoto Endo, Ladan Fazli, Jo Soden, Chris K Wang, Adam F Sander, Robert Dagil, Susan Thrane, Peter J Holst, Le Meng, Francesco Favero, Glen J Weiss, Morten A Nielsen, Jim Freeth, Torsten O Nielsen1, Joseph Zaia, Nhan L Tran, Jeff Trent, John S Babcook, Thor G Theander, Poul H Sorensen and Mads Daugaard. *Targeting human cancer by a glycosaminoglycan binding malaria protein.* Cancer Cell. 2015 Oct 12;28(4):500-14

Books or other non-periodical, one-time publications.

Nothing to report

Other publications, conference papers, and presentations.:

2013 Nordic Glycobiology Targeting Chondroitin-4-Sulfate in Cancer.

2014 Nordic Glycobiology Functional Characterization of an Oncofetal Chondroitin Sulfate Modification in Cancer

2014 The 9th European Workshop on Cell Death, Paphos, Cyprus. *Invited speaker.* Utilizing placental malaria tropism to target an oncofetal glycosaminoglycan structure.

2014 Ludwig Cancer Research, University of Oxford, UK. *Invited speaker.* . Utilizing placental malaria tropism to target an oncofetal glycosaminoglycan structure.

2014 Gordon research conference, July 6-11: Targeting of cancer-specific chondroitin sulfate A on circulating tumor cells using a evolutionary refined malaria protein National Annual PhD meeting in Oncology, March 26-27, 2014: Development of new diagnostic cancer methods using malaria proteins

2014 Medical University of Vienna, Vienna, Austria. *Invited speaker.* Utilizing placental malaria tropism to target an oncofetal glycosaminoglycan structure.

2015 The 10th Tuscany Retreat on Cancer Research – Novel treatment concepts in cancer. Tuscany, Italy. *Invited speaker.* Targeting oncofetal CSA in human cancer.

2015 Canadian Cancer Research Conference 2015. Montreal, Quebec, Canada. *Invited speaker.* Targeting a cancer-specific glycosaminoglycan modification using evolutionarily refined malaria proteins.

2015 National Annual PhD meeting in Oncology, April 15-16: Detection of circulating tumor cells using the malaria protein VAR2CSA

Technologies or techniques:

Nothing to report

Inventions, patent applications, and/or licenses:

The research builds upon patents that we submitted prior to the initiation of the grant.

Other Products:

Nothing to report

PARTICIPANTS & OTHER COLLABORATING ORGANIZATIONS

Name:	Ali Salanti (UCPH)
Person months:	6
Role:	PI
Support:	DoD, UCPH, ERC

Name:	Mads Daugaard (UBC)
Person months:	6
Role:	PI
Support:	DoD, UBC, PCC

Name:	Adam Sander (UCPH)
Person months:	3
Role:	Post doc
Support:	DoD, UCPH,

Name:	Reza Safaee (UBC)
Person months:	4

Role: Post doc
Support: DoD, UBC,

Name: Elham Alijazaeri (UCPH)
Person months: 12
Role: Lab tech
Support: DoD, UCPH,

Name: Dulguun Battsogt (UBC)
Person months: 12
Role: Research Assistant
Support: DoD, PCC

Has there been a change in the active other support of the PD/PI(s) or senior/key personnel since the last reporting period?

As the funding agency DoD is aware of, Mads Daugaard has changed affiliation from BCCRC to VPV in Canada. This has been approved by DoD and the grant has been transferred. It also meant that the funding period was prolonged; hence this is the final report from the UCPH part but not the VPC partner

What other organizations were involved as partners?

Nothing to report

SPECIAL REPORTING REQUIREMENTS

The report covers both the work done in the UCPH labs as well as in the VPC lab

APPENDICES:

Attached is the article describing the data presented in the report.

Article

Cancer Cell

Targeting Human Cancer by a Glycosaminoglycan Binding Malaria Protein

Graphical Abstract

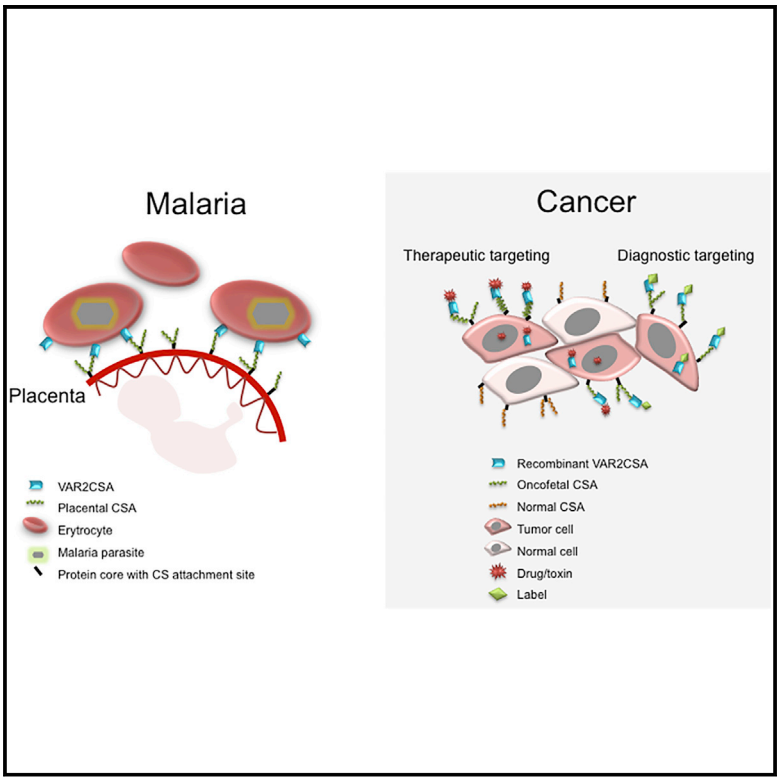

Authors

Ali Salanti, Thomas M. Clausen, Mette Ø. Agerbæk, ..., Thor G. Theander, Poul H. Sorensen, Mads Daugaard

Correspondence

salanti@sund.ku.dk (A.S.), mads.daugaard@ubc.ca (M.D.)

In Brief

The malarial protein VAR2CSA binds a placenta-specific chondroitin sulfate (CS). Salanti et al. show that the same CS is present in high fractions of cancer cells of many cancer types and that recombinant VAR2CSA conjugated with therapeutics strongly inhibit in vivo tumor growth.

Highlights

- The placenta and cancer express a similar type of oncofetal chondroitin sulfate
- Oncofetal chondroitin sulfate is displayed on proteoglycans in cancer
- Recombinant VAR2CSA proteins detect oncofetal chondroitin modifications
- Human cancer can be broadly targeted by malarial VAR2CSA drug conjugates in vivo

Salanti et al., 2015, Cancer Cell *28*, 500–514
October 12, 2015
http://dx.doi.org/10.1016/j.ccell.2015.09.003

CellPress

CellPress

Cancer Cell
Article

Targeting Human Cancer by a Glycosaminoglycan Binding Malaria Protein

Ali Salanti,[1,2,17,*] Thomas M. Clausen,[1,2,3,4,5,17] Mette Ø. Agerbæk,[1,2,3,4] Nader Al Nakouzi,[3,4] Madeleine Dahlbäck,[1,2] Htoo Z. Oo,[3,4] Sherry Lee,[3] Tobias Gustavsson,[1,2] Jamie R. Rich,[6,7] Bradley J. Hedberg,[6,7] Yang Mao,[8] Line Barington,[1,2] Marina A. Pereira,[1,2] Janine LoBello,[9] Makoto Endo,[10,11,12,13] Ladan Fazli,[3] Jo Soden,[14] Chris K. Wang,[3] Adam F. Sander,[1,2] Robert Dagil,[1,2] Susan Thrane,[1,2] Peter J. Holst,[1,2] Le Meng,[8] Francesco Favero,[15] Glen J. Weiss,[9,16] Morten A. Nielsen,[1,2] Jim Freeth,[14] Torsten O. Nielsen,[10,11] Joseph Zaia,[8] Nhan L. Tran,[9] Jeff Trent,[9] John S. Babcook,[6,7] Thor G. Theander,[1,2] Poul H. Sorensen,[5,18] and Mads Daugaard[3,4,18,*]

[1]Department of Immunology and Microbiology, Centre for Medical Parasitology, University of Copenhagen, 1014 Copenhagen, Denmark
[2]Department of Infectious Diseases, Copenhagen University Hospital, 2100 Copenhagen, Denmark
[3]Vancouver Prostate Centre, Vancouver, BC V6H 3Z6, Canada
[4]Department of Urologic Sciences, University of British Columbia, Vancouver, BC V5Z 1M9, Canada
[5]Department of Molecular Oncology, British Columbia Cancer Research Centre, Vancouver, BC V5Z 1L3, Canada
[6]Kairos Therapeutics, Inc., Vancouver, BC V6T 1Z3, Canada
[7]Centre for Drug Research and Development, Vancouver, BC V6T 1Z3, Canada
[8]Department of Biochemistry, Boston University School of Medicine, Boston, MA 02118, USA
[9]Translational Genomics Research Institute (TGen), Phoenix, AZ 85004, USA
[10]Genetic Pathology Evaluation Centre, University of British Columbia, Vancouver, BC V6H 3Z6, Canada
[11]Department of Pathology and Laboratory Medicine, University of British Columbia, Vancouver, BC V6T 2B5, Canada
[12]Department of Anatomic Pathology, Kyushu University, Fukuoka 812-8582, Japan
[13]Department of Orthopaedic Surgery, Kyushu University, Fukuoka 819-0395, Japan
[14]Retrogenix Ltd., Crown House, Bingswood Estate, Whaley Bridge, High Peak SK23 7LY, UK
[15]Centre for Biological Sequence Analysis, Technical University of Denmark, Lyngby 2800, Denmark
[16]Cancer Treatment Centers of America, Goodyear, AZ 85338, USA
[17]Co-first author
[18]Co-senior author
*Correspondence: salanti@sund.ku.dk (A.S.), mads.daugaard@ubc.ca (M.D.)
http://dx.doi.org/10.1016/j.ccell.2015.09.003

SUMMARY

Plasmodium falciparum engineer infected erythrocytes to present the malarial protein, VAR2CSA, which binds a distinct type chondroitin sulfate (CS) exclusively expressed in the placenta. Here, we show that the same CS modification is present on a high proportion of malignant cells and that it can be specifically targeted by recombinant VAR2CSA (rVAR2). In tumors, placental-like CS chains are linked to a limited repertoire of cancer-associated proteoglycans including CD44 and CSPG4. The rVAR2 protein localizes to tumors in vivo and rVAR2 fused to diphtheria toxin or conjugated to hemiasterlin compounds strongly inhibits in vivo tumor cell growth and metastasis. Our data demonstrate how an evolutionarily refined parasite-derived protein can be exploited to target a common, but complex, malignancy-associated glycosaminoglycan modification.

INTRODUCTION

When the malaria parasite, *Plasmodium falciparum,* replicates within infected erythrocytes, the latter become susceptible to clearance through the spleen. To avoid host clearance, the parasite expresses adhesion proteins on the surface of infected erythrocytes, which effectively anchor these cells to specific receptors in the host vasculature (Baruch et al., 1995). The anchor protein, VAR2CSA, mediates binding of infected erythrocytes to placental syncytiotrophoblasts (Salanti et al., 2003, 2004). This is

Significance

For decades researchers have sought to identify characteristics shared between placental or fetal development and cancer. This is based on the hypothesis that cancer cells, as part of their return to a less differentiated state, re-express genes involved in rapid growth and invasion during tissue development to facilitate cellular transformation and tumor progression. Using a specific placental glycan-binding malaria protein, we demonstrate that placental-like glycans are widely expressed in human tumors, with absent-to-low expression in normal tissues other than placenta. Furthermore, by conjugation of cytotoxic compounds to this protein, we demonstrate its capacity to specifically target cancer cells and block tumor growth in vivo.

the key event underlying placental malaria pathogenesis. In the placenta, VAR2CSA binds a distinct type of chondroitin sulfate (CS) glycosaminoglycan (GAG) chain called CS A (CSA) (Fried and Duffy, 1996). The minimal CS binding region of VAR2CSA consists of the Duffy Binding Ligand-like (DBL) 2X domain with flanking interdomain (ID) regions. This domain binds CS with remarkably high specificity and affinity (K_D ~15 nM) (Clausen et al., 2012; Dahlbäck et al., 2011).

CS is comprised of long linear polymers of repeated N-acetyl-D-galactosamine (GalNAc) and glucuronic acid (GluA) residues. These are present as modifications to proteoglycans (CSPGs) in the extracellular matrix (ECM) and in the cell plasma membrane. CSA chains are characterized by the presence of 4-*O*-sulfations (C4S) on the majority of the GalNAc residues of a given CS chain. Individual CSA chains show considerable variability with respect to the number of sulfated GalNAc residues, the density of sulfation modifications along the chain, as well as the chain length (Gama et al., 2006; Igarashi et al., 2013). *P. falciparum*-infected erythrocytes have been reported to bind CS oligosaccharides with 4-*O*-sulfated character (Alkhalil et al., 2000; Beeson et al., 2007). VAR2CSA expressing parasites only adhere in the placenta and do not bind to CS expressed elsewhere in the body (Fried and Duffy, 1996; Salanti et al., 2004). This suggests that placental CS, although incompletely resolved, is a distinct CS subtype expressed exclusively in the placenta. The function of placental-like CS (pl-CS) chains is not fully understood, but they are associated with the ability of trophoblasts to invade the uterine tissue and promote rapid cell proliferation as part of the normal placental implantation process (Baston-Büst et al., 2010). As proliferation and invasion are features shared with tumor cells, we hypothesized that placenta and cancer might express a similar type of CS. We explored the feasibility of using recombinant produced VAR2CSA proteins to target human cancer cells.

RESULTS

Recombinant Malarial VAR2CSA Detects a Distinct Placental-type CS

To examine the interaction between *P. falciparum*-infected erythrocytes and CS in the placenta, we developed an immunohistochemistry assay relying on the interaction between V5-tagged recombinant VAR2CSA (rVAR2) or control protein (rContr) (Figure 1A) and human tissue specimens. The rVAR2 protein efficiently bound both human and murine placental tissue, producing a grid-like staining pattern characteristic of plasma membrane binding, with no staining detected in normal tonsil control tissue (Figures 1B and S1A). Binding to placental tissues was completely inhibited by competition with purified CSA or by enzymatic removal of CS chains using chondroitinase AC, indicating that rVAR2 detects only pl-CS (Figure 1B). The majority of pl-CS was detected in the syncytiotrophoblast layer (Figure 1C, red arrows), with some staining in the underlying stromal cell compartment (Figures 1B and 1C). Staining with anti-C4S (2B6) revealed that CSA is abundant in most tissues despite the lack of rVAR2 staining. This confirms the tissue specificity of pl-CS (Figures 1D, S1B, and S1C). To evaluate the specific expression of pl-CS in other human tissues, we analyzed 20 different normal tissue types for their ability to bind rVAR2. While all tissues analyzed (other than placenta) displayed minimal to absent rVAR2 staining (Figure 1E), some tissues exhibited weak focal stromal staining not associated with cellular plasma membranes (Figure S1D). The choriocarcinoma cell line BeWo has been extensively used as a model for villous trophoblast function (Orendi et al., 2011). As expected, *P. falciparum*-infected human erythrocytes expressing VAR2CSA efficiently adhered to BeWo cells (Figure 1F, red arrows). Moreover, rVAR2 displayed strong binding to BeWo cells as measured by flow cytometry (Figure 1G), while primary endothelial, mesothelial, and embryonic kidney cells displayed low to absent binding of rVAR2 even at high concentrations (200 nM) (Figure 1H). Thus, in line with the fact that *P. falciparum*-infected VAR2CSA-expressing erythrocytes only sequester to the placenta, these data demonstrate that rVAR2 detects a distinct form of pl-CS expressed exclusively in the placenta and not on other normal cells or tissues.

pl-CS Is Expressed on Most Human Cancer Cells

The CSPG component of the placenta has been associated with the ability of the placental cells to maintain high proliferation rates and the capacity of the villous trophoblasts to invade into uterine tissue during implantation (Baston-Büst et al., 2010; Van Sinderen et al., 2013). Invasion and enhanced proliferation are phenotypes shared with cancer cells. We therefore hypothesized that the placental- and malignant compartments display a common CS signature that binds malarial VAR2CSA. Accordingly, we first showed that VAR2CSA expressing *P. falciparum*-infected erythrocytes displayed binding to human cancer cell lines in vitro, while no binding was observed to normal primary cells (Figure 2A). We next tested binding of rVAR2 to cancer cell lines and found that rVAR2 reacted with 95% (106/111) of patient-derived human cancer cell lines of hematopoietic, epithelial, and mesenchymal origin (Figures 2B–2E; Table S1). The interaction was rVAR2-concentration dependent and could be blocked by competition with soluble CSA (Figures 2B–2E and S2A). Furthermore, the affinity of rVAR2 binding to C32 melanoma cells was high and occurred with a K_D-value of 13 nM (Figure 2F). Also, VAR2CSA expressing *P. falciparum*-infected erythrocytes adhered to C32 cells and this interaction could be completely blocked by purified CSA (Figure 2G).

We next determined the specificity of the rVAR2-CSA interaction using ELISA as well as a flow cytometry-based competition assay on C32 cells. While all batches of rVAR2 (rVAR2-1, 2, and 3) efficiently bound immobilized CSPG molecules, no binding was observed to heparin sulfate PG (HSPG) or BSA as measured by ELISA (Figure S2B). Furthermore, pre-treating C32 cells with chondroitinase ABC reduced the rVAR2 binding to background levels (rContr) (Figures 2H–2J). The rVAR2-C32 interaction was also inhibited by purified free CSA in a dose-dependent manner (Figure 2H), whereas competition with the structurally similar 6-*O*-sulfated CS C (CSC) (Figure 2I) or highly charged heparan sulfate (HS) (Figure 2J) had limited effect on rVAR2 binding. Furthermore, while rVAR2 bound to the HS deficient CHO-pgsD-677, no binding was observed to CHO-S745A cells that have been selected for low xylosyltransferase activity and therefore low overall GAG content (Esko et al., 1985) (Figures S2C–S2E). Thus, human cancer and placental trophoblast cells express a common

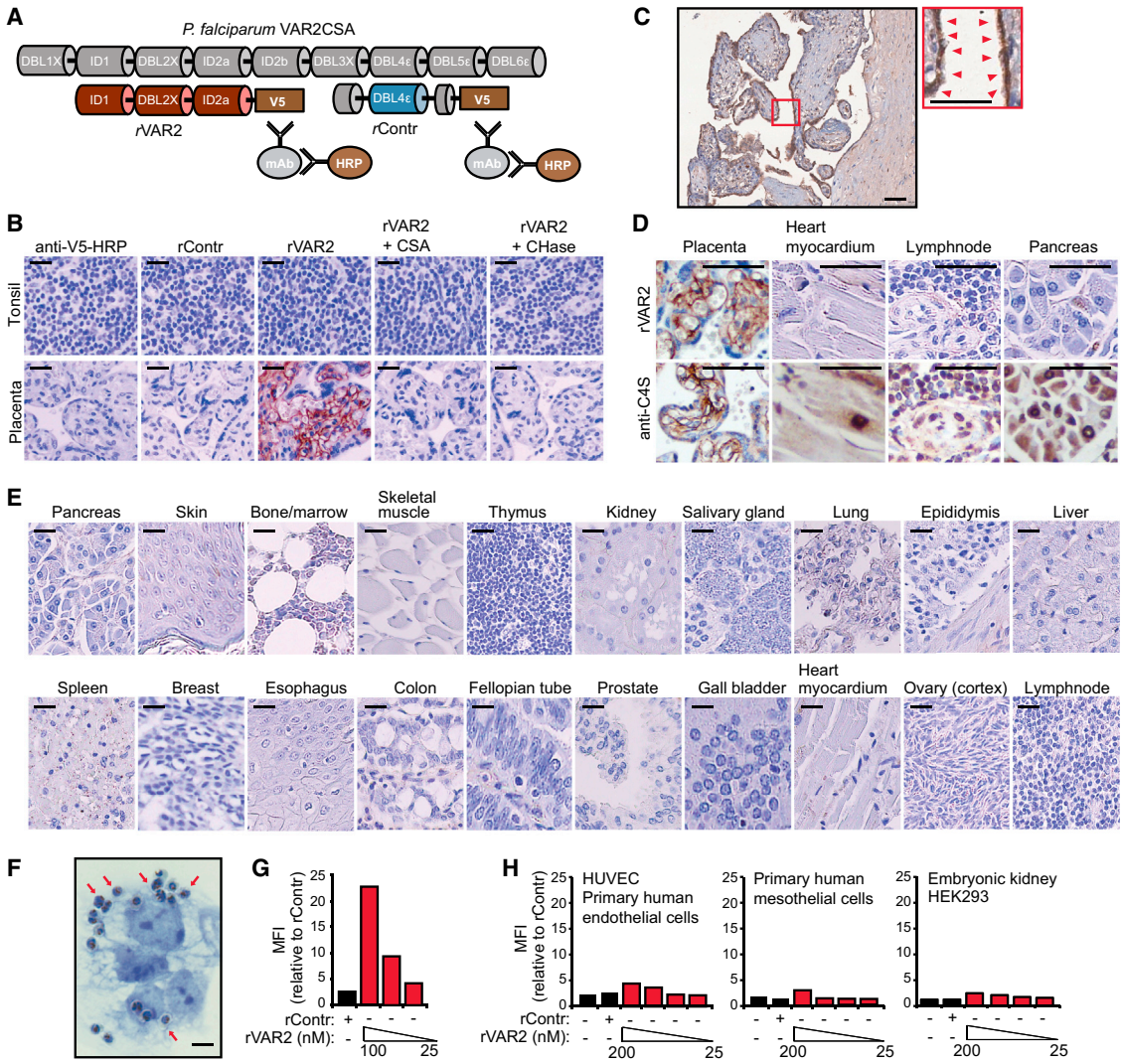

Figure 1. rVAR2 Detects a Distinct CS Modification in Human Placenta

(A) Schematic illustration of full-length *P. falciparum* VAR2CSA (gray), recombinant minimal CS-binding region (red), and recombinant non-CS binding region rContr (blue). The antibodies toward the C-terminal V5 tag are used to detect rVAR2.

(B) Representative images of indicated tissue specimens incubated with anti-V5 + anti-mouse-HRP alone (anti-V5-HRP) or in combination with recombinant rContr or rVAR2 with or without chondroitinase ABC (CHase ABC) or purified CSA. The scale bar represents 20 μm.

(C) Human placenta tissue stained as in (B), red arrows indicate pl-CS on the syncytium. The scale bars represent 10 μm.

(D) The denoted tissues stained for total CSA using enzymatic GAG end-processing and anti-C4S (2B6) antibody or for CS detected by rVAR2 as in (B). The scale bar represents 10 μm.

(E) A selection of 20 normal tissues stained as in (B). The scale bar represents 20 μm.

(F) Representative image of *P. falciparum*-infected, VAR2CSA-expressing erythrocytes bound to the plasma membrane (red arrows) of trophoblastic BeWo cells. The scale bar represents 1 μm.

(G) Relative mean fluorescence intensity (MFI) of trophoblastic BeWo cells incubated with recombinant rContr or rVAR2 as indicated and detected by flow cytometry using anti-V5-FITC.

(H) HUVECs, human primary mesothelial cells, and human embryonic kidney cells (HEK293) analyzed as in (G).

See also Figure S1.

and distinct form of CS, which can be specifically recognized by recombinant malarial VAR2CSA.

De novo CSA synthesis involves several enzymes (Sugahara et al., 2003). While B3GAT1 is required for synthesis of the basal GlcA-Gal-Gal-Xyl-Ser linker tetrasaccharide common to all GAGs, CSGALNACT1 commits the GAG to the CS pathway. Within the CS maturation pathway, CHST11 mediates CSA-specific 4-*O*-sulfation of the GalNAc residues of the CS chain (Figure 2K). Furthermore, the sulfation level of CSA is balanced by the 4-*O*-sulfatase ARSB, which removes C4S from the CSA chains (Litjens et al., 1989). RNAi-mediated knock down of B3GAT1, CSGALNACT1, and CHST11 expression inhibited the

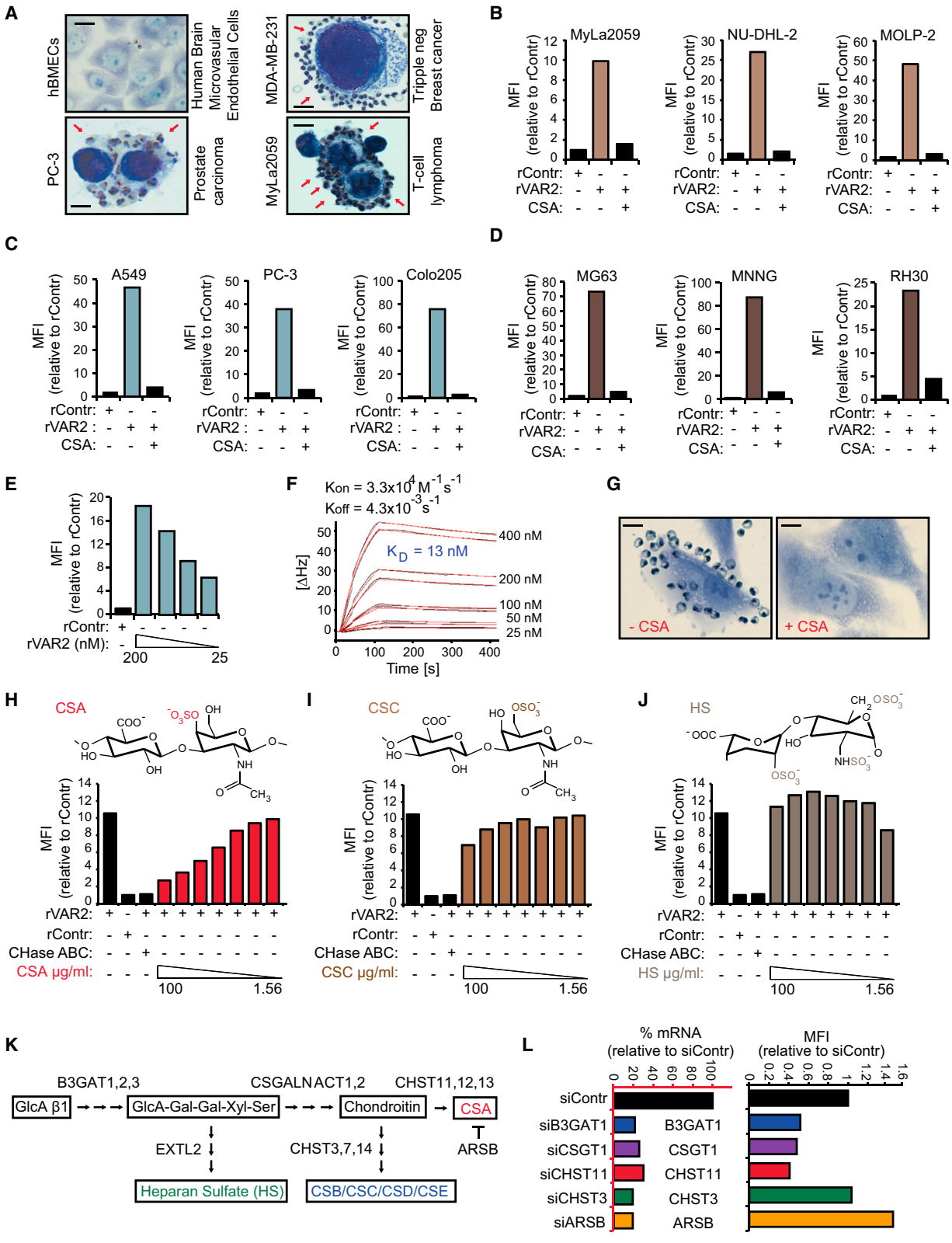

Figure 2. rVAR2 Detects pl-CS on Cancer Cells

(A) Representative images of indicated normal primary cells (hBMECs) and tumor cells (PC-3, MDA-MB-231, and MyLa2059) with adherence *P. falciparum*-infected, VAR2CSA-expressing human erythrocytes (red arrows). The scale bar represents 1 μm.

(legend continued on next page)

binding of rVAR2 to U2OS cells, while knock down of CHST3, an enzyme involved in 6-*O*-GalNAc sulfation, had no effect on binding (Figure 2L). Knock down of ARSB increased the binding of rVAR2 (Figure 2L), indicating that 4-*O*-sulfated CS residues constitute an important component of the pl-CS GAG chain.

To confirm the clinical relevance of CS expression, we analyzed available expression data from lung cancer patients linked to therapeutic outcome for expression of the key enzymes involved in CSA synthesis (B3GAT1, CSGALNACT1, and CHST11). While the expression pattern of enzymes required for synthesis of the CS GAG backbone (B3GAT1 and CSGALNACT1) had no predictive value in lung cancer, high expression of the enzyme specifically required for CSA 4-*O*-sulfation (CHST11) significantly correlated with poor relapse-free survival in three independent lung cancer cohorts (Figure S2F). The same pattern was observed for breast and colon cancer (Figure S2F). Together, these data indicate that major human cancers induce expression of a CS chain, which likely consists predominantly of GalNAc residues.

pl-CS Is Widely Expressed in Primary Human Cancer

To extend these findings to human tumor specimens, we examined a panel of human epithelial tumors for rVAR2 binding as compared to adjacent normal tissue from the same patients, using the same methods as in Figures 1B–1E. Although differences in pl-CS staining intensity were observed among the different subtypes and tumor stages, all tumors displayed strong rVAR2 binding and only weak staining in matched normal tissue (Figure 3A). The staining pattern indicates that pl-CS may be expressed on both epithelial tumor cells and tumor-associated stromal cells. Binding of rVAR2 to primary human tumors could be completely inhibited by competing with soluble CSA chains or by enzymatic removal of CS from the tissue (Figure 3B). Moreover, pl-CS was not restricted to epithelial tumors, as rVAR2 also strongly reacted with mesenchymal soft-tissue and bone sarcomas (Figure 3C).

We then analyzed 676 malignant tumors from patients with localized stage I–III invasive ductal breast carcinoma (n = 124), stage IIb bone sarcomas (n = 20), and stage I–III soft-tissue sarcomas (n = 532). Ranking the staining-intensity on a 0–3 scale (where 2 equals the staining intensity of the placenta) revealed that ~90% of the breast tumors, ~80% of the bone sarcomas, and ~85% of soft-tissue sarcoma specimens studied showed positive staining for pl-CS on the plasma membrane or in the tumor stroma (Figures 3D, S3A, and S3B). Of all the sarcoma subtypes investigated, only Ewing sarcomas showed weak or absent binding of rVAR2 in the majority of cases (Figure 3D). To investigate whether the weak binding of rVAR2 to Ewing sarcomas was due to a general lack of CS chains or a specific lack of pl-CS, we analyzed a tissue microarray (TMA) of 47 Ewing sarcoma specimens in triplicates from adult and pediatric patients. The TMA was subjected to staining with three different CS reagents, rVAR2, 2B6 (binding C4S following Chondroitinase ABC treatment), and CS56 (binding C4S and C6S) (Figures S3C–S3E). This analysis showed that 80.6% of all Ewing sarcoma cases were positive for at least one of the three reagents, while rVAR2 stained ~39% of the Ewing specimens (Figure S3F). These data suggest that Ewing sarcomas display a broad selection of CS chains, but only a fraction of these are placental-type CS that can be bound by rVAR2. Moreover, while many low-risk mesenchymal neoplasms (including lipoma, fibromatosis, neurofibroma, Schwannoma, and pigmented villonodular synovitis) displayed absent or low-to-moderate staining for pl-CS, the majority of malignant lesions showed strong staining (Figure S3G).

With a tool to broadly target pl-CS chains in primary human cancer, we next analyzed whether this malignancy-associated CS alteration was linked to progression or outcome of malignant disease. We analyzed an available melanoma progression TMA (n = 159) for expression of pl-CS. While the majority of benign nevi displayed an absent or low pl-CS expression, the presence of pl-CS in the tumor microenvironment increased significantly in Clark 2–5 staged melanoma ($p = 0.000056$) and in metastatic/recurrent disease ($p = 0.000058$) (Figure 3E; Table S2). These data suggest that pl-CS is a candidate marker for disease progression in melanoma. We subsequently investigated whether pl-CS detected by rVAR2 was associated with outcome in human non-small cell lung cancer. Analysis of a TMA comprised of 165 primary tumors linked to outcome demonstrated that high expression of pl-CS correlated with poor relapse-free survival of the patients ($p = 0.016$) (Figures S3H and S3I). Collectively, these data demonstrate that highly diverse human malignant tumor types originating from distinct germ layers display a common distinct pl-CS signature that predicts disease progression and outcome (summarized in Figure 3F).

Molecular Characterization and Expression of Placenta-like CS

To better define the rVAR2 binding of CS from cancer cells, we extracted GAGs from different cancer cell types followed

(B–D) Relative mean fluorescence intensity (MFI) of representative hematological (B), epithelial (C), or mesenchymal (D) lineage human cancer cell lines incubated with recombinant rContr or rVAR2 in combination with soluble CSA as indicated and detected by flow cytometry using anti-V5-FITC.

(E) C32 human melanoma cells incubated with recombinant rContr or indicated concentrations of recombinant rVAR2 analyzed as in (B).

(F) Sensorgram showing binding between recombinant VAR2CSA and immobilized C32 cells measured in delta Hertz [ΔHz] as a function of time (s) using the indicated concentrations of recombinant protein. The black lines represent data and the red lines represent fitted curves attained by a 1:1 binding model. The affinity is given as K_D values calculated from K_{on} and K_{off}.

(G) Representative images of C32 melanoma cells flushed over with *P. falciparum*-infected human erythrocytes in absence ($^-$CSA) or presence ($^+$CSA) of soluble CSA. The scale bar represents 1 μm.

(H–J) Relative mean fluorescence intensity (MFI) of C32 melanoma cells incubated with recombinant rContr or rVAR2 in combination with chondroitinase ABC (CHase ABC), soluble CSA, (H), CSC (I), or HS (J) as indicated and detected by flow cytometry using anti-V5-FITC.

(K) Schematic illustration of key enzymatic events in the CS synthesis pathway.

(L) rVAR2 binding (black bars, right) and RT-PCR readout of mRNA levels (blue bars, left) of U2OS cells transfected with control (C), B3GAT1 (B3), CSGALNACT1 (CSG), CHST11 (C11), CHST3 (C3), or ARSB (AB) siRNAs.

See also Figure S2 and Table S1.

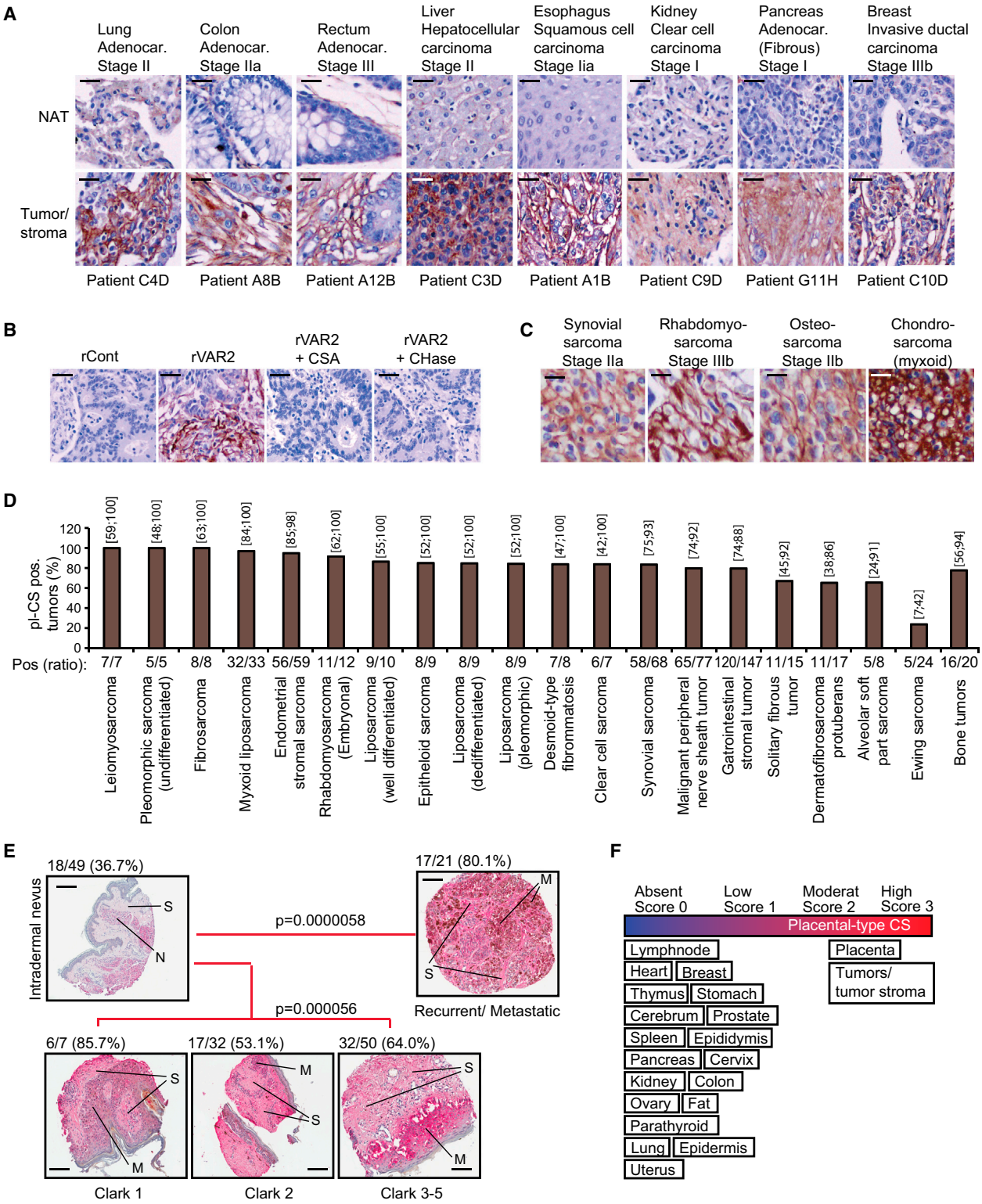

Figure 3. Diverse Types of Human Cancer Express pl-CS

(A) Representative images of indicated patient-matched primary tumor and normal adjacent tissue (NAT) specimens stained with rVAR2-V5 and detected by anti-V5-HRP. The scale bar represents 10 μm.

(B) Representative images of stage IIa breast tumors stained with rContr or rVAR2 as in (A) with or without soluble CSA or chondroitinase ABC (CHase ABC). The scale bar represents 10 μm.

(legend continued on next page)

by rVAR2 affinity purification, structural analysis using tandem mass spectrometry (tandem-MS), and affinity analysis using Attana's biosensor technology and flow cytometry. MS of GAG extracts showed that bovine trachea CSA (BT-CSA) was 10% un-sulfated and 90% mono-sulfated (no di-sulfation detected), whereas cancer-associated CS was 98% mono-sulfated (Figure 4; Table S3). Furthermore, tandem-MS revealed that BT-CSA mono-sulfated population contained 79.6% C4S and 20.4% of C6S, while CS from Myla2059 lymphoma cells contained 69.8% C4S and 30.2% C6S (Figure 4B, left). Although rVAR2 binding to cancer cells and tissue was outcompeted by BT-CSA, high amounts (100–400 μg/ml) were required to fully disrupt the rVAR2-cancer cell interaction (Figures 2B–2D). This indicated that rVAR2 only bound a fraction of the CSA chains present in the crude BT-CSA preparation. To investigate this, we affinity purified BT-CSA and MyLa2059 CS extract on an rVAR2 column (Figure 4B, right) and characterized it by MS. BT-CSA affinity purification on rVAR2 resulted in mono-sulfated CS that was enriched (90%) for C4S (Figure 4B; Table S3). Compared to bulk BT-CSA, the BT-CSA eluted from the column was considerably more effective in competitively inhibiting the binding between rVAR2 and C32 melanoma cells as measured by flow cytometry (Figure 4C), as well as the binding of rVAR2 to immobilized CSPG measured by the biosensor (Figure 4D). CS from MyLa2059 cells affinity purified on rVAR2 columns inhibited binding of rVAR2 to immobilized CSPG with an IC_{50} of 0.033 μg/ml compared to 0.063 μg/ml for placenta CS and 0.79 μg/ml for BT-CSA (Figures 4D and S4A–S4C; Table S4).

Placental cells, human melanoma cells, and some breast cancer and glioma cells have been found to express high levels of the CSA-modified proteoglycan, CSPG4 (Van Sinderen et al., 2013; Wang et al., 2010). To test whether CSPG4 carries pl-CS that can be bound by rVAR2, we analyzed co-localization and direct interaction between rVAR2 and CSPG4 on C32 melanoma cells. The rVAR2 stain co-localized with CSPG4 (Figure 4E) and specifically pulled down CS-conjugated CSPG4 from C32 melanoma cells (Figure 4F). However, rVAR2 could also bind tumor cells negative for CSPG4 expression (compare Figures 4G and 2B–2E), suggesting that pl-CS can be displayed on other CPSG protein cores. To identify these, we transfected non-malignant HEK293 cells (which do not bind rVAR2) with 3,500 different human plasma membrane proteins (Figure 4H). Following validation with CSA competition and enzymatic removal of CS chains by chondroitinase treatment, it was evident that 17 of the 3,500 proteins facilitated binding to rVAR2 (Figure 4H). Thus, in addition to CSPG4 (not included in the screen), at least 17 proteins including CD44, carbonic anhydrase IX (CA9), syndecan 1 (SDC1), or tomoregulins (TMEFF1 and -2) can carry pl-CS when overexpressed in HEK cells. Further studies are required to investigate if all of the proteoglycans can be modified with CS in vivo. Interestingly, ten of these proteins have previously been described as being conditional CS-conjugated and 15 have been directly associated with human malignant disease (Table S5). To investigate the inter-tumor diversity in expression of proteoglycans able to display pl-CS, we analyzed 1,555 primary human tumor specimens representing 17 major types of human cancers using the Bittner array (Rhodes et al., 2004) and the Riker melanoma array (Riker et al., 2008). This analysis showed that the proteoglycans associated with pl-CS were differentially, but complementarily, expressed in each of the 17 major cancer groups tested (Figures 4I and S4D). Accordingly, we validated the interaction of rVAR2 with the CS-modified form of CD44 in C32 melanoma cells (Figure 4J). Moreover, rVAR2 efficiently pulled down glycosylated CD44 from C32 melanoma protein lysates (Figure 4K). Together, these data suggest that rVAR2 can be utilized to broadly target pl-CS chains in human malignancies with different proteoglycan expression profiles.

Internalization and In Vivo Localization of rVAR2

The specific presence of a pl-CS modification in malignant tumors suggests that VAR2CSA may be utilized to deliver cytotoxic payloads directly to the tumor microenvironment. We first investigated if rVAR2 is internalized upon binding to tumor cells. Alexa488-labeled rVAR2 (rVAR2-A488) (Figure 5A) rapidly bound to human colon cancer cells (Colo205) and was efficiently internalized within 30 min (Figures 5B and 5C). Similar internalization dynamics were observed with three other cancer cell lines (Figure 5D). We then investigated if rVAR2 was able to sequester to tumors in vivo. To visualize rVAR2 tumor sequestration, we conjugated an Alexa750 near-infra red (NIR) fluorescent probe to rVAR2 (rVAR2-NIR) (Figure 5E, top). The rVAR2-NIR was administrated IV into PC-3 tumor bearing mice and a NIR signal from the tumor region was observed after 10 min in vivo and ex vivo (Figure 5E, bottom). Moreover, ex vivo analysis of fixed PC-3 xenografts confirmed strong rVAR2 reactivity in the tumors as measured by immunohistochemistry (Figure 5F). Similarly, we injected the rVAR2-NIR IV into B16-tumor bearing mice and followed the rVAR2-NIR signal for 48 hr. As in the PC3 xenograft, rVAR2 rapidly located to the tumor and the signal was detectable 48 hr after injection (Figures 5G and 5H). Together, these data suggest that rVAR2 can be utilized to facilitate intracellular delivery of cytotoxic compounds to pl-CS expressing cells in vivo.

Targeting Tumors through the rVAR2 pl-CS Signature

To test whether rVAR2 could be used as a pl-CS-specific tumor targeting system, we genetically fused the cytotoxic domain of Diphtheria toxin (DT388) to rVAR2, creating a recombinant rDT388-VAR2 (rVAR2-DT) fusion protein (Figure 6A). In vitro, the rVAR2-DT protein efficiently killed tumor cell lines of both

(C) Representative images of indicated soft-tissue and bone sarcomas stained with rContr or rVAR2 as in (A). The scale bar represents 5 μm.
(D) Column graph representation of pl-CS staining intensity in the indicated soft-tissue and bone sarcoma subtypes (n = 552) processed as in (A) and scored (0–3) for binding to recombinant VAR2CSA. The columns show the percentage and exact binomial 95% confidence interval of pl-CS positive (score 2–3) tumors.
(E) Representative images of a melanoma progression TMA stained with anti-V5-HRP in combination with recombinant rVAR2 and scored (0–3). The fraction of score 2–3 (moderate/high) pl-CS (pl-CS) positive tumors was identified and p values were generated by the Goodman-Kruskal-Gamma test (Nevus, N; Stroma, S; and Melanoma cells, M). The scale bar represents 40 μm.
(F) Schematic representation of pl-CS expression in the indicated tissue categories.
See also Figure S3 and Table S2.

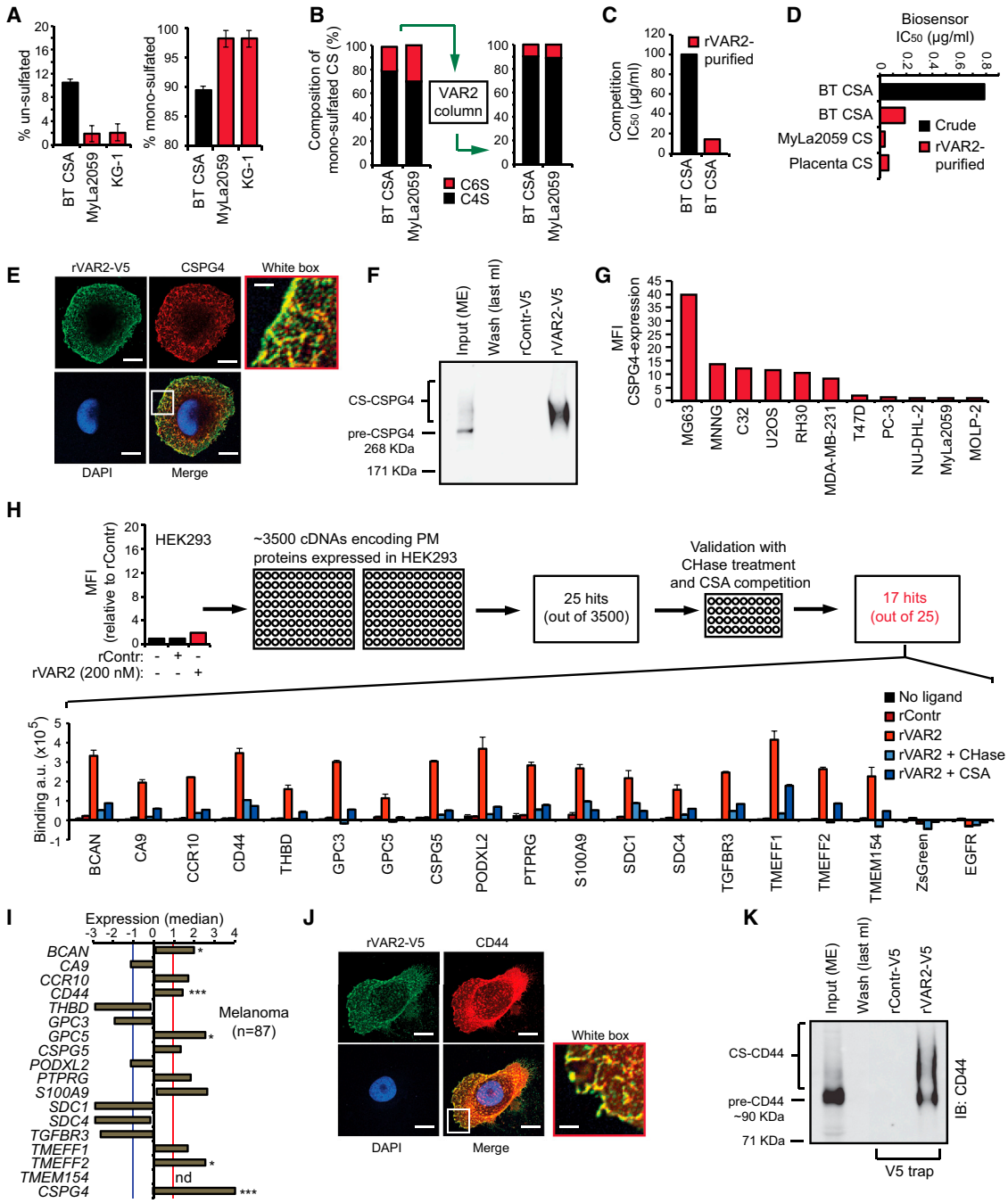

Figure 4. Defining the rVAR2 CS Epitope

(A) Level of un-sulfated (left) and mono-sulfated (right) disaccharides of extracted CS from Sigma BT-CSA, T cell lymphoma (MyLa2059), and myeloid leukemia (KG-1) determined by liquid chromatography MS analysis. The values are given as a percentage of the total CS in the sample.

(B) BT-CSA and MyLa2059 CSA were affinity purified on a custom made rVAR2 column and eluted in a NaCl gradient. The composition of the mono-sulfated CS was analyzed by tandem MS before (left) and after (right) affinity purification.

(C) Binding inhibition capacity of BT-CSA before and after rVAR2 affinity purification is shown as the concentration needed to block 50% of the binding (IC_{50} values) between rVAR2 and the cells as measured by flow cytometry.

(D) Biosensor analyses of the capacity of BT-CSA (before and after rVAR2 affinity purification) and rVAR2 affinity-purified Myla2059 and placental CS, to inhibit rVAR2 binding to immobilized CSPG. The binding inhibition is shown as the concentration needed to block 50% of the binding (IC_{50} values) between rVAR2 and the cells.

(E) Representative picture of a C32 human melanoma cell co-stained for CS using rVAR2-V5 (green) and CSPG4 (red). The co-localization was analyzed by confocal microscopy. The scale bar represents 0.5 µm.

(legend continued on next page)

epithelial and mesenchymal origin (Figures 6B and 6C) with low IC_{50} values (from 0.8 nM to 12.2 nM). The rVAR2-DT toxin had no effect on normal primary human endothelial cells (HUVEC) (Figure 6C), and competition with CSA abolished the cytotoxic effect of rVAR2-DT on cancer cells (Figure 6B). Moreover, small interfering (si)RNAs targeting C4S-sulfotransferase CHST11 or the CS backbone-conjugation enzyme CSGALNACT1 prevented the cytotoxic effects of rVAR2-DT in prostate cancer PC-3 cells (Figures 6D and 6E). These data demonstrate that the C4S conjugation machinery is required for rVAR2 to deliver a cytotoxic payload to tumor cells.

Prostate cancer is a leading cause of morbidity and death among men in the Western world, and the prognosis for advanced castration resistant prostate cancer (CRPC) is poor (Kirby et al., 2011). We therefore tested the efficacy of rVAR2-DT in a mouse tumor xenograft model based on the metastatic CRPC cell line, PC-3. As few as three doses of rVAR2-DT were able to significantly inhibit growth of PC-3 CRPC tumors in vivo (Figure 6F). We next performed independent experiments to assess the longer-term effect of three doses of rVAR2-DT on CRPC growth in vivo. The rVAR2-DT treated group was monitored for tumor growth for up to 20 days after the first dose. Similar to the first setup (Figure 6F), we observed a strong inhibition of tumor growth in the rVAR2-DT treated group (Figure 6G). Interestingly, the inhibitory effect of rVAR2-DT on tumor growth persisted 14 days after first dose (10 days after last dose), before slow re-growth of the tumor was observed (day 14, blue arrows) (Figure 6G). The PC-3 cells used in the study expressed luciferase, allowing us to monitor the impact of rVAR2-DT on PC-3 xenografts by IVIS. Scanning of the mice at day 3 and day 13 after the initial dose fully corroborated the results from Figures 6F and 6G and showed marked inhibition of chemiluminiscence within the treated group (Figure 6H). Histopathology analysis revealed dramatic differences between rVAR2-DT treated and un-treated tumors. While the vehicle control displayed intact and dense tumor architecture with little necrosis (Figure 6I), rVAR2-DT treated tumors showed massive necrosis (Figure 6J), similar to what is seen in the liver after wild-type DT delivery (Saito et al., 2001). Furthermore, rVAR2-DT treated xenografts were also positive for TUNEL staining indicative of apoptosis (Figure 6K). Examination of kidney and liver tissues from the rVAR2-DT treated animals showed normal tissue architecture and no morphologic signs of toxicity (Figures 6L and 6M). These data demonstrate that rVAR2 can facilitate efficacious CS-dependent delivery of a cytotoxic compound to CRPC tumors in vivo with no morphologic evidence of adverse effects on normal tissues.

Development and Efficacy of an rVAR2-Hemiasterlin Drug Conjugate

From the human clinical trials with DT fusions, it is apparent that high drug concentrations are not well tolerated. We therefore chemically conjugated a hemiasterlin analog (KT886) to rVAR2 via a protease cleavable linker (Figure S5), utilizing free cysteines in the recombinant protein (Figures 7A and 7B). The rVAR2-KT886 drug conjugate (VDC886) carried an average of three toxins per rVAR2 molecule (Figure 7B). ELISA, biosensor, and flow cytometry confirmed the affinity and specificity of VDC886 to pl-CS. A total of 33 cancer cell lines of different origin were tested for sensitivity to VDC886. All lines were effectively killed in vitro by the VDC886, with IC_{50} values ranging from 0.2 pM to 30 nM (Figure 7C). We performed a dose escalation study of VDC886 in healthy female CD-1 mice, increasing the dose up to 15 mg/kg. The maximum tested dose of 15 mg/kg was well tolerated, and the animals did not display any signs of morbidity or physical distress. Histopathology examination of different organs did not show any evidence of adverse cytotoxic effects (Figure 7D). Importantly, the pl-CS modification was present in the murine placenta (Figure S1), as well as on murine tumor cells (Figures 5D, 5G, 7H, and 7K), indicating that the absence of adverse effects was not due to lack of pl-CS expression capability in the murine system. We subsequently tested the efficacy of the VDC886 in vivo using two different human xenograft mouse models of non-Hodgkin's lymphoma (Karpas299) and prostate cancer (PC-3). VDC886 treatment significantly inhibited growth of both Karpas299 (Figure 7E) and PC-3 (Figure 7F) tumors as compared to the control groups. Remarkably, two out of six mice in the VDC886-treated PC-3 tumor group showed complete remission 32 days after the first treatment (Figure 7G). These data demonstrate that VDC886 can target diverse human tumor types in vivo. To further analyze the anti-tumor effects of pl-CS targeting in vivo, we made use of a highly aggressive syngeneic (immunocompetent) mouse model of metastatic murine breast cancer cells. 4T1 breast cancer cells were efficiently

(F) Extracted membrane proteins (Input ME) from C32 melanoma cells were subjected to an on-column pulldown on a HiTrap NHS column coupled with rVAR2-V5 or rControl-V5. The figure shows Input (ME), last 1 ml of wash of the rVAR2-V5 column, and the 0.5 M NaCl elution following concentration. The samples were analyzed for precipitation of precursor (pre-CSPG4) and CSA-conjugated CSPG4 by immunoblotting (IB:CSPG4) as indicated.

(G) Relative mean fluorescence intensity (MFI) of indicated cell lines incubated with anti-CSPG4 antibody and detected by flow cytometry.

(H) Relative mean fluorescence intensity (MFI) of HEK293 cells incubated with recombinant rContr or rVAR2 as indicated and detected by flow cytometry using anti-V5-FITC. The HEK293 cells were transfected with 3,500 cDNAs encoding known tumor-associated plasma membrane proteins inserted in a ZsGreen expression system and analyzed for their ability to facilitate binding to recombinant rVAR2 detected by anti-V5-Alexa647. The column graph displays quantified anti-V5-Alexa647 detection (arbitrary units, a.u.) in HEK293 cells transfected with the indicated plasma membrane proteins and left un-treated (no ligand), or treated with recombinant rContr, rVAR2 alone, or in combination with chondroitinase ABC (rVAR2 + CHase) or purified CSA (rVAR2 + CSA).

(I) Median expression compared to overall average of the genes encoding the 17 proteins from (H) plus CSPG4 in primary melanoma (n = 87) patient specimens extracted from the Oncomine Riken melanoma array (*$p < 0.05$ and ***$p < 0.001$) (not determined: nd) (missing probe). The red and blue cross-lines designate the threshold for up and downregulated.

(J) Representative picture of a C32 human melanoma cell co-stained for CS using rVAR2-V5 (green) and CD44 (red). The co-localization was observed by confocal microscopy. The scale bar represents 0.5 μm.

(K) Extracted membrane proteins (Input ME) from C32 melanoma cells were subjected to an on-column pulldown on a HiTrap NHS column coupled with rVAR2-V5 or rControl-V5. The figure shows Input (ME), last 1 ml of wash of the rVAR2-V5 column, and the 0.5 M NaCl elution following up-concentration. The samples were analyzed for precipitation of precursor (pre-CD44) and CS-conjugated CD44 by immunoblotting (IB:CD44) as indicated. The error bars indicate ± SD.
See also Figure S4 and Tables S3–S5.

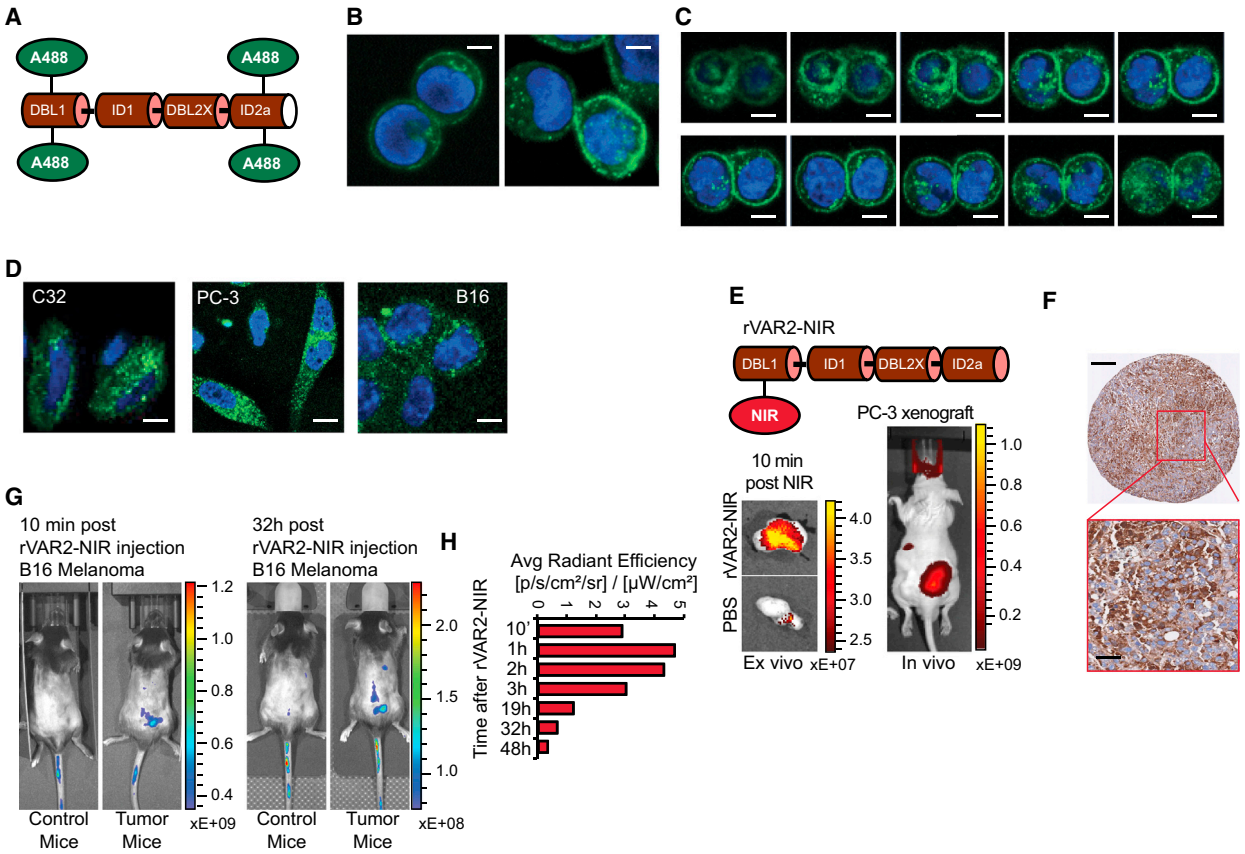

Figure 5. rVAR2 Internalization and In Vivo Tumor Localization

(A) Schematic illustration of rVAR2 conjugated with Alexa-488 (rVAR2-A488).

(B) Colo205 colon carcinoma cells analyzed by confocal microscopy 5 (left) and 30 (right) min after addition of rVAR2-FITC (green) and DAPI (blue). The scale bar represents 0.5 μm.

(C) Confocal microscopy analysis of Colo205 cells as in (B) displayed as vertical depth at 30 min after addition of rVAR2-FITC. The scale bar represents 0.5 μm.

(D) C32 melanoma, PC-3 prostate adenocarcinoma, and B16 murine melanoma cells analyzed as in (B) 30 min after addition of rVAR2-FITC. The scale bar represents 0.5 μm.

(E) Schematic illustration of rVAR2 conjugated with NIR Alexa-750 (rVAR2-NIR) probe (upper) and in vivo (right) and ex vivo (left) detection of NIR signal in PC-3 tumor xenografts 10 min post-rVAR2-NIR injection in tail vein.

(F) IHC of PC-3 tumor xenografts stained with rVAR2-V5 and detected by anti-V5-HRP. The scale bar represents 40 μm.

(G) C57BL/6 mice with no tumors (Control mice) or carrying established B16 murine melanoma tumors (Tumor mice) were injected with rVAR2-NIR in the tail vein at day 10 and scanned in an IVIS Spectrum CT scanner.

(H) Quantification of IVIS signal from a subcutaneous B16 tumor (right flank) after rVAR2-NIR injection at different time intervals from 10 min to 48 hr. The right flank signal is considered as background and is *subtracted from the initial signal*.

bound by rVAR2 in a concentration and CSA-dependent manner (Figure 7H). Moreover, VDC886 demonstrated strong cytotoxicity in 4T1 cells in vitro, which could be completely rescued by competition with soluble CSA (Figure 7I). Injection of luciferase-4T1 cells in the left ventricle of the heart of C57BL/6 mice resulted in aggressive bone metastasis with an overall penetrance of 50%–60% (Figure 7J). The bone metastases invaded into adjacent muscle and showed strong pl-CS expression as analyzed by rVAR2-based immunohistochemistry (IHC) (Figure 7K). Notably, of the mice with 4T1 bone metastases, five out of six mice in the VDC886-treated group were still alive at the end of the study (day 54) with no detectable metastases, while all control-treated mice died with metastatic disease ($p = 0.0196$; Figures 7L and 7M). Indeed, VDC886-treatment significantly increased survival of mice with 4T1 bone metastasis as compared to control-treated mice. Collectively, these data provide compelling evidence that diverse human and murine tumor types can be effectively targeted in vivo using an rVAR2 drug conjugate.

DISCUSSION

The placenta is a fast-growing organ in which cells display high mitotic rates, the ability to invade the uterine tissue, and the capacity to establish an elaborate vasculature. These are features shared with cancer, and hence researchers have for decades attempted to identify molecules shared between the placental and malignant compartments (Holtan et al., 2009). We have demonstrated that recombinant versions of the evolutionarily refined malaria protein VAR2CSA can broadly

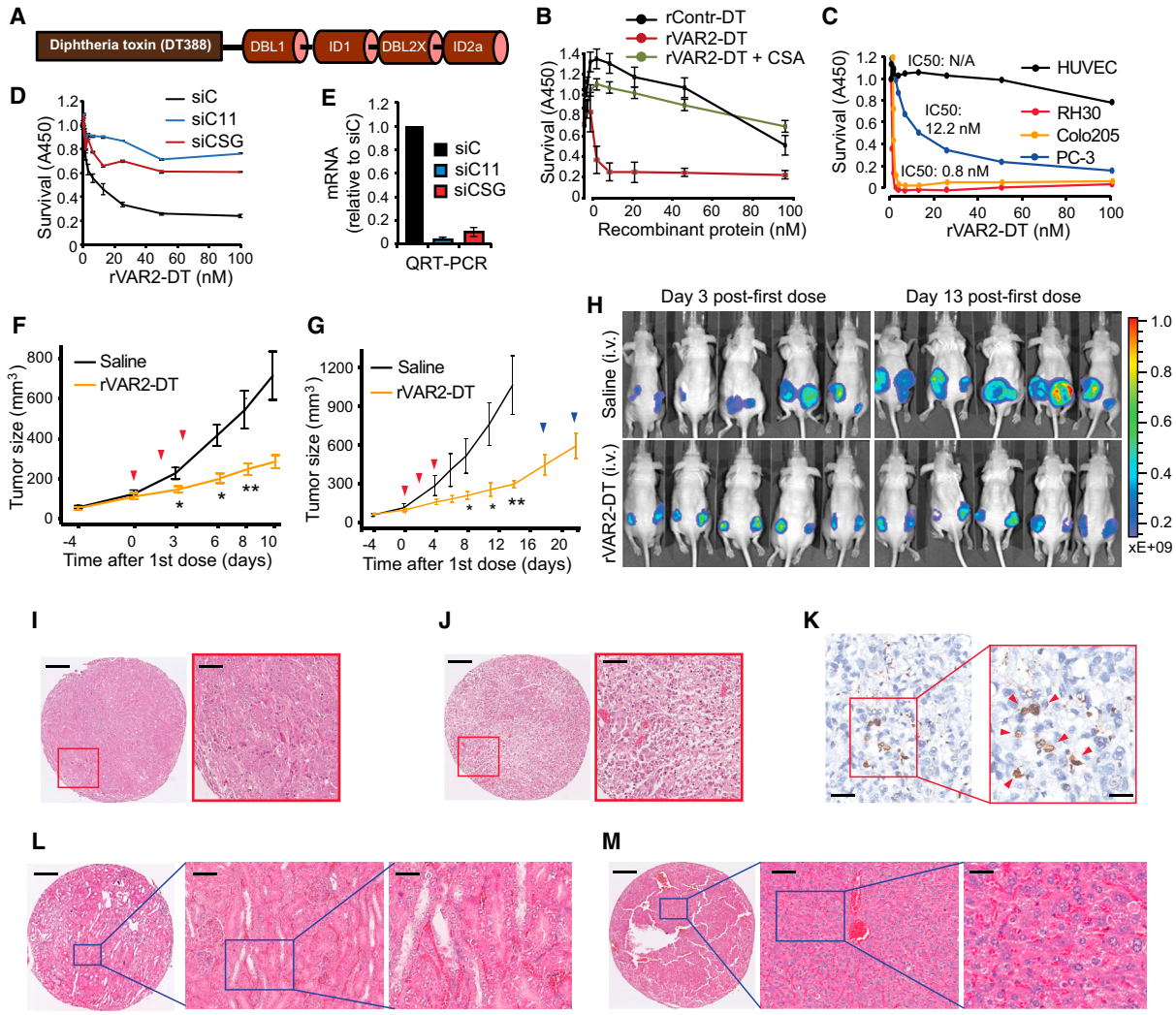

Figure 6. In Vivo Cancer Targeting Using rVAR2 Fusion Construct rVAR2-DT388

(A) Schematic figure showing the architecture of the rVAR2-DT388 fusion protein.

(B) Survival of B16 melanoma cells treated with increasing concentrations (0–100 nM) of a DT-fused (rContr-DT) or rVAR2-DT with or without CSA competition as indicated and analyzed for WST1 staining 96 hr post-treatment. The error bars indicate ± SD.

(C) Survival of indicated cell lines treated with increasing concentrations (0–100 nM) of rVAR2-DT.

(D) PC-3 cells were transfected with control siRNA (siC) or siRNAs targeting CHST11 (siC11) or CSGALNACT1 (siCSG) and treated with the indicated concentrations (0–100 nM) of rVAR2-DT for 96 hr before analyzed for survival using methylene blue staining assay. The error bars indicate ± SD.

(E) Quantitative RT-PCR of indicated mRNA levels in PC-3 cells after 72 hr post-transfection with control siRNA (siC), CSGALNACT1 siRNA (siCSG), and CHST11 siRNA (siC11). The error bars indicate ± SD.

(F and G) Quantification of tumor volume over 10 days (Experiment 1, F) and 20 days (Experiment 2, G) in Foxn1^{nu} mice xenotransplated with PC-3 cells and treated on day 0, 2, and 4 (red arrows) with either saline (black line) or 0.6 mg/kg rVAR2-DT (yellow line) (*$p < 0.05$ and **$p < 0.01$). The error bars indicate ± SEM.

(H) IVIS analysis of PC-3 tumor growth in mice (from G) on day 3 and 13 post-first dose treatment with saline or rVAR2-DT as indicated.

(I and J) Representative hematoxylin and eosin (H&E) images as indicated of PC-3 xenograft tumor after treatment with saline (I) or rVAR2-DT (J). The scale bar represents 40 μm.

(K) Representative image of PC-3 xenograft tumor stained with TUNEL reagent (in 20× and 40× magnification as indicated). The scale bar represents 10 μm (left) and 5 μm (right).

(L and M) Representative H&E images as indicated of kidney (L) and liver (M) extracted from rVAR2-DT treated mice in (G). The scale bar represents 40 μm.

detect pl-CS on trophoblastic cells as well as in human tumors.

The broad targeting potential of rVAR2 is likely facilitated by the redundant presentation of pl-CS chains on several different cancer-associated PGs such as CSPG4 and CD44. Several of the PGs that carry an rVAR2-reactive CS chain are currently being, or have been, tested as targets in clinical trials (Casucci et al., 2013; Wang et al., 2011). We propose that targeting the common CS chain present on different cancer-associated PGs may potentially offer a broad cancer targeting strategy.

Since rVAR2 is efficiently internalized into pl-CS expressing cells, rVAR2 could potentially facilitate the delivery of anti-cancer

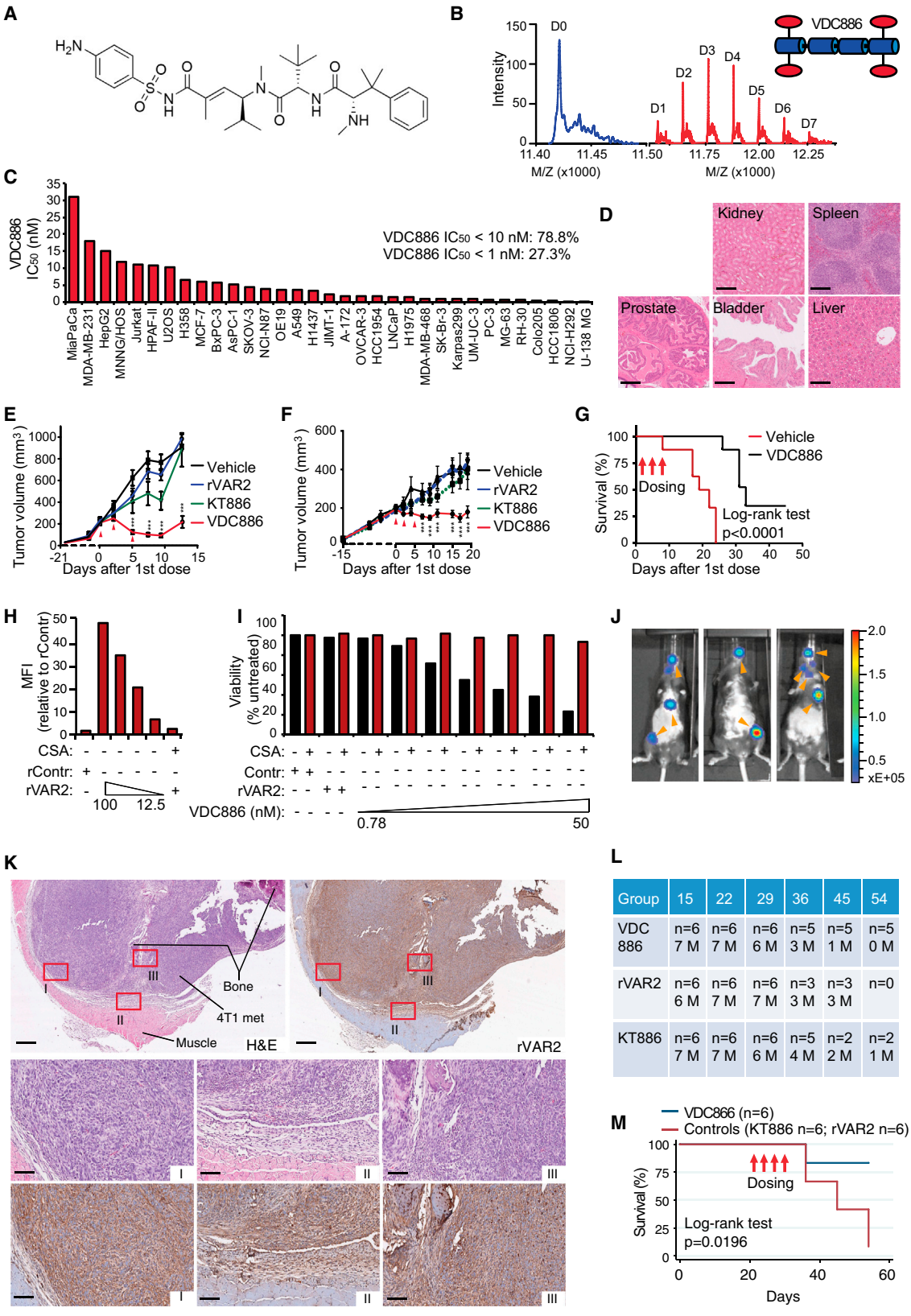

Group	15	22	29	36	45	54
VDC 886	n=6 7 M	n=6 7 M	n=6 6 M	n=5 3 M	n=5 1 M	n=5 0 M
rVAR2	n=6 6 M	n=6 7 M	n=6 7 M	n=3 3 M	n=3 3 M	n=0
KT886	n=6 7 M	n=6 7 M	n=6 6 M	n=5 4 M	n=2 2 M	n=2 1 M

(legend on next page)

compounds directly into the tumor environment. This notion was supported by our in vivo and ex vivo imaging experiments. We subsequently demonstrated the therapeutic potential of targeting pl-CS on human tumors by two different approaches. First, rVAR2 genetically fused to a part of the diphtheria toxin (rVAR2-DT), efficiently killed tumor cells in vitro and in vivo in a CS-dependent manner. Second, chemical conjugation of a hemiasterlin toxin to rVAR2 created a highly potent VDC886 that specifically targeted pl-CS on diverse tumor cells in vitro and in vivo. Notably, non-pregnant mice injected with rVAR2-DT or VDC886 showed no adverse treatment effects, suggesting that pl-CS is expressed below rVAR2–based detection levels in non-malignant tissue in mammals. This is supported by the observation that *P. falciparum*-infected erythrocytes cannot bind anywhere in vascularized tissue compartments, except in the placenta.

Our data promote pl-CS as a candidate target for broad rVAR2-based anti-cancer therapies, as well as a progression marker for selected human tumor types such as melanoma. rVAR2 provides an example of how evolutionarily refined host-pathogen anchor molecules can be conveniently exploited to access and target cancer associated glycans.

EXPERIMENTAL PROCEDURES

Reagents and Cell Culture

The recombinant proteins were expressed in SHuffle T7 Express Competent *E. coli* (NEB) and purified using HisTrap from GE Healthcare, followed by size exclusion chromatography. Purified CSA, HS, and chondroitinase ABC were obtained from Sigma. CSC was obtained from Seikagaku, and Monoclonal anti-V5 and anti-V5-FITC antibodies were obtained from Invitrogen. Cells were transfected with siRNAs (QIAGEN) (10 nM final) against B3GAT1, CSGALNACT1, CHST11, CHST3, or ARSN using RNAiMAX (Invitrogen) and analyzed for rVAR2 binding by flow cytometry and for mRNA expression by RT-PCR.

IHC

Using the Ventana Discovery platform, sectioned paraffin-embedded tissue samples were stained with 500 picomolar V5-tagged rVAR2 without antigen retrieval, followed by 1:700 monoclonal anti-V5 step and a anti-mouse-HRP detection step. For a detailed description, please see Supplemental Information.

Flow Cytometry

Cells were grown to 70%–80% confluency in appropriate growth media and harvested in an EDTA detachment solution (Cellstripper). Cells were incubated with protein (200–25 nM) in PBS containing 2% fetal bovine serum (FBS) for 30 min at 4°C and binding was analyzed in a FACSCalibur (BD Biosciences) after a secondary incubation with an anti-V5-FITC antibody. For inhibition studies, protein was co-incubated with indicated concentration of GAGs (CSA, CSC, and HS).

Binding Kinetics Analysis

A quartz crystal microbalance biosensor (Attana Cell A200, Attana AB) was used for the kinetic analyses. Cells were seeded onto cell compatible sensor chips and incubated 24 hr at 37°C. Cells were then fixed in 3.7% formaldehyde and visualized using DAPI. The data, including k_{on}, k_{off}, and the calculated K_D, were presented as sensorgrams showing VAR2CSA fragments binding to cells as response (in Hertz) as a function of time (s). Curve fitting was performed in the Attache evaluation software (Attana AB).

Immunocytochemistry

Internalization Assay

rVAR2 protein was conjugated with the Alexa488 fluorophore according to the manufacturer's instructions. C32 cells were seeded to coverslips and grown to 60% confluency. There were 200 nM rVAR2-488 that were incubated with the cells for 1 hr at 4°C and then washed once to allow internalization of only surface-bound protein at either 10 min or 60 min at 37°C. Cells were subsequently washed with PBS prior to fixation with 4% paraformaldehylde for 15 min at room temperature. Coverslips were mounted in mounting media containing DAPI and analyzed by laser-scanning confocal microscopy.

Co-localization

C32 melanoma cells were grown on glass cover slides. Cells were fixed in 4% paraformaldehyde (PFA), blocked in 1% BSA/ 5% FBS, and stained for CS

Figure 7. In Vivo Cancer Targeting Using VDC886

(A) Structure of the hemiasterlin analog KT886.

(B) MS readout confirming KT886 loading on rVAR2 through a toxin-linker functionalized with a maleimide group to enable conjugation to protein-thiols. The D0 (blue) represents un-conjugated rVAR2 and D1-7 (red) designates the number of KT886 loaded. The VDC886 carries 3.5 KT886 toxins on average.

(C) Indicated human cancer cell lines were seeded in 96-well plates and treated with VDC886 in concentrations ranging from 0.01 pM to 1 μM. The column graph displays IC_{50} kill-values of VDC886 performance.

(D) Representative H&E images as indicated of kidney, spleen, prostate, bladder, and liver extracted from mice subjected to three doses of VDC886 on alternating days (15 mg/kg). The scale bar represents 10 μm.

(E) Female C.B-17/IcrHsd-Prkdc scid mice engrafted with Karpas299 non-Hodgkin's lymphoma cells on the back were treated with 1× PBS (vehicle), naked rVAR2 (rVAR2), KT886 alone (KT886), or VDC886. The treatments were administered intravenously on day 0, 2, and 5 (red arrows) as indicated.

(F) Male Foxn1^{nu} mice were implanted subcutaneously on the back with the PC3 prostate cancer cell line in 100 μl of Matrigel (in both right and left flanks). The test articles, as in (E), were administered intravenously on day 0, 2, and 5 (red arrows) as indicated. The animals remained on study until their combined tumor burden reached 1,000 mm^3 in size or they otherwise required euthanasia due to distress (humane endpoint).

(G) Kaplan-Meier curve of Vehicle and VDC886 treated mice from (F). There were two of the six mice on study in the VDC886 treated group that had complete re-mission of disease (***$p < 0.001$).

(H) 4T1 murine breast cancer cells were analyzed by flow cytometry for binding to the indicated concentrations of rVAR2 or 100 nM rContr in the absence or presence of soluble CSA.

(I) The indicated concentration range of VDC886 was tested on 4T1 murine mammary cancer cells in the absence or presence of soluble CSA as indicated.

(J) Detection of bone metastasis detectable by IVIS (orange arrows) in C57BL/6 mice 2–3 weeks after injected with luciferase-expressing 4T1 cells from (H) and (I) in the left ventricle of the heart.

(K) Extracted bone metastasis from (J) subjected to matched H&E staining and immunohistochemical pl-CS staining using rVAR2-V5 + anti-V5-HRP as indicated. The lower image displays the sections within red boxes (from upper). The scale bar represents 1 mm (upper) and 50 μm (lower).

(L) Mice as in (J) with bone metastasis visible in the same IVIS detection range (n = 18) were randomized into three groups with six mice per group (n = 6) and subjected to four doses of VDC886 (15 mg/kg), rVAR2 alone (rVAR2), or KT886 alone (KT886) in equivalent molar ratios to VDC886 on day 21, 24, 27, and 30. All groups were monitored on day 15, 22, 29, 36, 45, and 54 as indicated for number of mice (n) and number of visible metastasis (M).

(M) Kaplan-Meier survival plot of (L), comparing the two control groups (rVAR2 and KT886) combined with VDC886 treated mice. The mice were sacrificed when reaching their humane endpoint. The red arrows designate dosing days. The p value was calculated with Chi2 log-rank test. The error bars represent ± SEM. See also Figure S5.

using rVAR2-V5 and CSPG4 (LHM2, Abcam) or CD44 (2C5, RnD Systems) overnight at 4°C. rVAR2 was detected by anti-V5 (Rabbit) and anti-Rabbit-Alexa488. CSPG4 and CD44 antibodies were detected with anti-mouse-Alexa568. Nuclei were stained with DAPI. Slides were analyzed by laser-scanning confocal microscopy.

CS Extraction from Cancer Cells

Myla-2059 T cell lymphoma and KG-1 leukemia cells were grown to 1 × 10^6 cells/ml in supplemented RPMI-1620. A total of 500 × 10^6 cells (Myla-2059 and KG-1) were pelleted and the pellet was treated with Trypsin-EDTA (Lonza), containing 1 mM NaSO4, for 30 min at 37°C. The supernatant was cleared of cells and the GAGs were extracted by ion exchange chromatography. Briefly, the supernatant was loaded onto a Q FF sepharose column (GE), the column was washed in 200 mM NaCl, and finally the GAGs were eluted in 1.5 M NaCl. The GAG's were precipitated overnight (O/N) at 4°C in two volumes of ethanol and the precipitate was collected by centrifugation.

Purification of CS on a VAR2 Column

There were 1.5 mg rVAR2 (DBL1-ID2a) that were immobilized onto a Hitrap NHS HP Column (GE). The column was inactivated with ethanolamine and washed in PBS. Sigma CSA or Myla-2059 GAG extract was adjusted to 1 × PBS and loaded onto the column in five passages. The column was washed in PBS and the bound GAG eluted at 0.25 M NaCl, 0.5 M NaCl, 1 M NaCl, and 2 M NaCl in succession. The eluted GAGs were precipitated in ethanol O/N at 4°C in two volumes of ethanol and the precipitate was collected by centrifugation. The eluted fractions were tested for their ability to inhibit rVAR2 binding to CSPG (Attana) and C32 cancer cells (Flow Cytometry, see above).

Disaccharide Analysis of CS

The disaccharide compositions of CS samples were analyzed using chondroitinase ABC and size exclusion chromatography-MS (SEC-MS) as previously described (Shi and Zaia, 2009). Each type of CS disaccharides was extracted from the total ion chromatogram (TIC), integrated, and quantified by comparing with an external standard containing known amount of CS disaccharides. The sulfation position for the monoly-sulfated disaccharides was determined by tandem-MS experiments using previously established methods (Shao et al., 2013). The diagnostic fragment ions for the 4-*O*-sulfated disaccharide (Y_1, *m/z* 300.0484) and for 6-*O*-sulfated disaccharide (Z_1, *m/z* 282.0362) were extracted from the TIC, counted, and compared with a standard curve generated using commercial standards.

Biosensor Affinity Analysis

The analysis of the purified GAG species was performed on a quartz crystal microbalance biosensor (Attana A100, Attana AB). CSPG (Decorin, Sigma) was coupled to a LNB carboxyl chip using EDC and Sulfo-NHS. The chip was inactivated with ethanolamine. The sensor chips were inserted into the machine and allowed to stabilize in PBS running buffer, at 25°C using a flow rate of 25 μl per min. rVAR2 (30 nM) was mixed with a titration of inhibitor and injected onto the surface. Control rVAR2 was run repeatedly during analysis to account for changes in the binding surface. The binding surface was re-generated after each test injection with injections of 0.25% SDS in PBS. Peak response levels were recorded using the Attester Evaluation software (Attana AB) and presented as a ratio to the nearest rVAR2 injection. IC_{50} values were calculated in Excel.

IVIS In Vivo Imaging

rVAR2 was NIR labeled through available amines with an Alexa750 Succinimidyl ester (Invitrogen). This was done with an excess of NIR probe (10× molar) according to the manufacturer's instructions. The coupled protein was injected (4 mg/kg) IV in the tail vein of healthy and tumor bearing mice 10 days post-establishment of a subcutaneous B16 melanoma tumor in the right flank. The mice were scanned using an IVIS spectrum CT scanner (Perkin Elmer). Scanning was done at time intervals ranging from 10 min to 48 hr. In vivo tumor signal quantification is presented as an absolute signal in reference to the signal of the flank of the healthy control mouse. Data analysis was performed using the Living Image Software (Caliper Life Sciences).

Patient Material

All human specimens were collected under full consent and according to the guidelines set forth and approved by the University of British Columbia (UBC) human ethics committee.

In Vivo Studies

The methodologies described were re-viewed and approved by the Institutional Animal Care Committee (IACC) at the University of British Columbia and the animal experiments inspectorate at the University of Copenhagen prior to conducting the study. During the study the care, housing, and use of animals was performed in accordance with the Canadian Council on Animal Care Guidelines and the Danish animal experiments inspectorate guidelines. For a detailed description of the in vivo studies and tolerability studies please see the Supplemental Information section.

SUPPLEMENTAL INFORMATION

Supplemental Information includes Supplemental Experimental Procedures, five figures, and five tables and can be found with this article online at http://dx.doi.org/10.1016/j.ccell.2015.09.003.

AUTHOR CONTRIBUTIONS

M.D., A.S., T.G.T., T.M.C., J.S.B., and P.H.B.S. designed the research; T.M.C., M.Dahlbäck, M.Ø.A., T.G., N.A.N., C.K.W., S.L., H.Z.O., L.F., M.E., J.S., L.B., F.F., M.A.N., J.F., Y.M., L.M., J.L., R.D., S.T., M.A.P., J.R.R., and B.J.H. performed the experiments; T.O.N., N.L.T., J.T., G.J.W., J.Z., P.J.H., and A.F.S. provided useful reagents and helpful discussions; and A.S., P.H.B.S., T.G.T., T.M.C., and M.D. wrote the manuscript.

ACKNOWLEDGMENTS

The authors are thankful to Dr. Chao Sima at TGen, Phoenix, AZ, for assistance with TMA-related bioinformatics; Dr. Jeffrey Allen formerly of University of Tennessee Health Science Center, Memphis, TN, currently at Humboldt Medical Specialists, Eureka, CA for lung cancer tissue access and assistance with clinical annotation; Birita Fritleifsdottir for help with B16 xenograft model; and Monika Stints and Thomas Lavstsen for hBMEC cells. We would like to acknowledge the contributions of Geoffery Winters, Alex Mandel, Tom Hseih, Peter Bergqvist, Lawrence Amankwa, Siobhan O'Brien, Faisal Pany, Eric Cruz, and Natalia Neverova for their work on the rVAR2 drug conjugate at The Centre for Drug Research and Development.

The work was supported by funds from the Novo Nordisk Foundation; the Danish Cancer Society; and Stand Up To Cancer – St. Baldrick's Pediatric Dream Team Translational Research Grant (SU2C-AACR-DT1113). Stand Up To Cancer is a program of the Entertainment Industry Foundation administered by the American Association for Cancer Research; Augustinus Foundation; U.S. Department of Defense (DoD); the Harboe Foundation; the European Research Councils (ERC) through the MalOnco program; The Danish Innovation Foundation; VAR2 Pharmaceuticals; Kairos Therapeutics; the Spar Nord Foundation; Team Finn and other riders in the Ride to Conquer Cancer; Safeway; and the Prostate Cancer Canada (PCC) Foundation. A.S., M.D., T.G.T., and P.H.S. are shareholders of VAR2 Pharmaceuticals ApS and members of the board of directors. J.R., B.H., and J.B. are employees of Kairos Therapeutics, Inc. J.F. and J.S. are employees of Retrogenix Ltd.

Received: June 12, 2015
Revised: July 31, 2015
Accepted: September 8, 2015
Published: October 12, 2015

REFERENCES

Alkhalil, A., Achur, R.N., Valiyaveettil, M., Ockenhouse, C.F., and Gowda, D.C. (2000). Structural requirements for the adherence of Plasmodium falciparum-infected erythrocytes to chondroitin sulfate proteoglycans of human placenta. J. Biol. Chem. *275*, 40357–40364.

Baruch, D.I., Pasloske, B.L., Singh, H.B., Bi, X., Ma, X.C., Feldman, M., Taraschi, T.F., and Howard, R.J. (1995). Cloning the P. falciparum gene encoding PfEMP1, a malarial variant antigen and adherence receptor on the surface of parasitized human erythrocytes. Cell *82*, 77–87.

Baston-Büst, D.M., Götte, M., Janni, W., Krüssel, J.S., and Hess, A.P. (2010). Syndecan-1 knock-down in decidualized human endometrial stromal cells leads to significant changes in cytokine and angiogenic factor expression patterns. Reprod. Biol. Endocrinol. *8*, 133.

Beeson, J.G., Andrews, K.T., Boyle, M., Duffy, M.F., Choong, E.K., Byrne, T.J., Chesson, J.M., Lawson, A.M., and Chai, W. (2007). Structural basis for binding of Plasmodium falciparum erythrocyte membrane protein 1 to chondroitin sulfate and placental tissue and the influence of protein polymorphisms on binding specificity. J. Biol. Chem. *282*, 22426–22436.

Casucci, M., Nicolis di Robilant, B., Falcone, L., Camisa, B., Norelli, M., Genovese, P., Gentner, B., Gullotta, F., Ponzoni, M., Bernardi, M., et al. (2013). CD44v6-targeted T cells mediate potent antitumor effects against acute myeloid leukemia and multiple myeloma. Blood *122*, 3461–3472.

Clausen, T.M., Christoffersen, S., Dahlbäck, M., Langkilde, A.E., Jensen, K.E., Resende, M., Agerbæk, M.O., Andersen, D., Berisha, B., Ditlev, S.B., et al. (2012). Structural and functional insight into how the Plasmodium falciparum VAR2CSA protein mediates binding to chondroitin sulfate A in placental malaria. J. Biol. Chem. *287*, 23332–23345.

Dahlbäck, M., Jørgensen, L.M., Nielsen, M.A., Clausen, T.M., Ditlev, S.B., Resende, M., Pinto, V.V., Arnot, D.E., Theander, T.G., and Salanti, A. (2011). The chondroitin sulfate A-binding site of the VAR2CSA protein involves multiple N-terminal domains. J. Biol. Chem. *286*, 15908–15917.

Esko, J.D., Stewart, T.E., and Taylor, W.H. (1985). Animal cell mutants defective in glycosaminoglycan biosynthesis. Proc. Natl. Acad. Sci. USA *82*, 3197–3201.

Fried, M., and Duffy, P.E. (1996). Adherence of Plasmodium falciparum to chondroitin sulfate A in the human placenta. Science *272*, 1502–1504.

Gama, C.I., Tully, S.E., Sotogaku, N., Clark, P.M., Rawat, M., Vaidehi, N., Goddard, W.A., 3rd, Nishi, A., and Hsieh-Wilson, L.C. (2006). Sulfation patterns of glycosaminoglycans encode molecular recognition and activity. Nat. Chem. Biol. *2*, 467–473.

Holtan, S.G., Creedon, D.J., Haluska, P., and Markovic, S.N. (2009). Cancer and pregnancy: parallels in growth, invasion, and immune modulation and implications for cancer therapeutic agents. Mayo Clin. Proc. *84*, 985–1000.

Igarashi, N., Takeguchi, A., Sakai, S., Akiyama, H., Higashi, K., and Toida, T. (2013). Effect of molecular sizes of chondroitin sulfate on interaction with L-selectin. Int. J. Carbohydr. Chem. *2013*, 9.

Kirby, M., Hirst, C., and Crawford, E.D. (2011). Characterising the castration-resistant prostate cancer population: a systematic review. Int. J. Clin. Pract. *65*, 1180–1192.

Litjens, T., Baker, E.G., Beckmann, K.R., Morris, C.P., Hopwood, J.J., and Callen, D.F. (1989). Chromosomal localization of ARSB, the gene for human N-acetylgalactosamine-4-sulphatase. Hum. Genet. *82*, 67–68.

Orendi, K., Kivity, V., Sammar, M., Grimpel, Y., Gonen, R., Meiri, H., Lubzens, E., and Huppertz, B. (2011). Placental and trophoblastic in vitro models to study preventive and therapeutic agents for preeclampsia. Placenta *32* (*Suppl*), S49–S54.

Rhodes, D.R., Yu, J., Shanker, K., Deshpande, N., Varambally, R., Ghosh, D., Barrette, T., Pandey, A., and Chinnaiyan, A.M. (2004). ONCOMINE: a cancer microarray database and integrated data-mining platform. Neoplasia *6*, 1–6.

Riker, A.I., Enkemann, S.A., Fodstad, O., Liu, S., Ren, S., Morris, C., Xi, Y., Howell, P., Metge, B., Samant, R.S., et al. (2008). The gene expression profiles of primary and metastatic melanoma yields a transition point of tumor progression and metastasis. BMC Med. Genomics *1*, 13.

Saito, M., Iwawaki, T., Taya, C., Yonekawa, H., Noda, M., Inui, Y., Mekada, E., Kimata, Y., Tsuru, A., and Kohno, K. (2001). Diphtheria toxin receptor-mediated conditional and targeted cell ablation in transgenic mice. Nat. Biotechnol. *19*, 746–750.

Salanti, A., Staalsoe, T., Lavstsen, T., Jensen, A.T., Sowa, M.P., Arnot, D.E., Hviid, L., and Theander, T.G. (2003). Selective upregulation of a single distinctly structured var gene in chondroitin sulphate A-adhering Plasmodium falciparum involved in pregnancy-associated malaria. Mol. Microbiol. *49*, 179–191.

Salanti, A., Dahlbäck, M., Turner, L., Nielsen, M.A., Barfod, L., Magistrado, P., Jensen, A.T., Lavstsen, T., Ofori, M.F., Marsh, K., et al. (2004). Evidence for the involvement of VAR2CSA in pregnancy-associated malaria. J. Exp. Med. *200*, 1197–1203.

Shao, C., Shi, X., White, M., Huang, Y., Hartshorn, K., and Zaia, J. (2013). Comparative glycomics of leukocyte glycosaminoglycans. FEBS J. *280*, 2447–2461.

Shi, X., and Zaia, J. (2009). Organ-specific heparan sulfate structural phenotypes. J. Biol. Chem. *284*, 11806–11814.

Sugahara, K., Mikami, T., Uyama, T., Mizuguchi, S., Nomura, K., and Kitagawa, H. (2003). Recent advances in the structural biology of chondroitin sulfate and dermatan sulfate. Curr. Opin. Struct. Biol. *13*, 612–620.

Van Sinderen, M., Cuman, C., Winship, A., Menkhorst, E., and Dimitriadis, E. (2013). The chrondroitin sulfate proteoglycan (CSPG4) regulates human trophoblast function. Placenta *34*, 907–912.

Wang, X., Wang, Y., Yu, L., Sakakura, K., Visus, C., Schwab, J.H., Ferrone, C.R., Favoino, E., Koya, Y., Campoli, M.R., et al. (2010). CSPG4 in cancer: multiple roles. Curr. Mol. Med. *10*, 419–429.

Wang, X., Katayama, A., Wang, Y., Yu, L., Favoino, E., Sakakura, K., Favole, A., Tsuchikawa, T., Silver, S., Watkins, S.C., et al. (2011). Functional characterization of an scFv-Fc antibody that immunotherapeutically targets the common cancer cell surface proteoglycan CSPG4. Cancer Res. *71*, 7410–7422.

Cancer Cell, Volume *28*

Supplemental Information

Targeting Human Cancer by a Glycosaminoglycan Binding Malaria Protein

Ali Salanti, Thomas M. Clausen, Mette Ø. Agerbæk, Nader Al Nakouzi, Madeleine Dahlbäck, Htoo Z. Oo, Sherry Lee, Tobias Gustavsson, Jamie R. Rich, Bradley J. Hedberg, Yang Mao, Line Barington, Marina A. Pereira, Janine LoBello, Makoto Endo, Ladan Fazli, Jo Soden, Chris K. Wang, Adam F. Sander, Robert Dagil, Susan Thrane, Peter J. Holst, Le Meng, Francesco Favero, Glen J. Weiss, Morten A. Nielsen, Jim Freeth, Torsten O. Nielsen, Joseph Zaia, Nhan L. Tran, Jeff Trent, John S. Babcook, Thor G. Theander, Poul H. Sorensen, and Mads Daugaard

SUPPLEMENTAL DATA

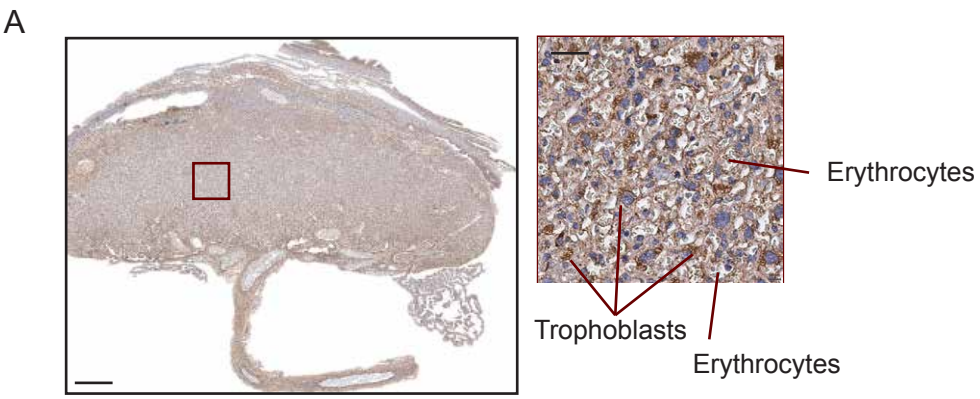

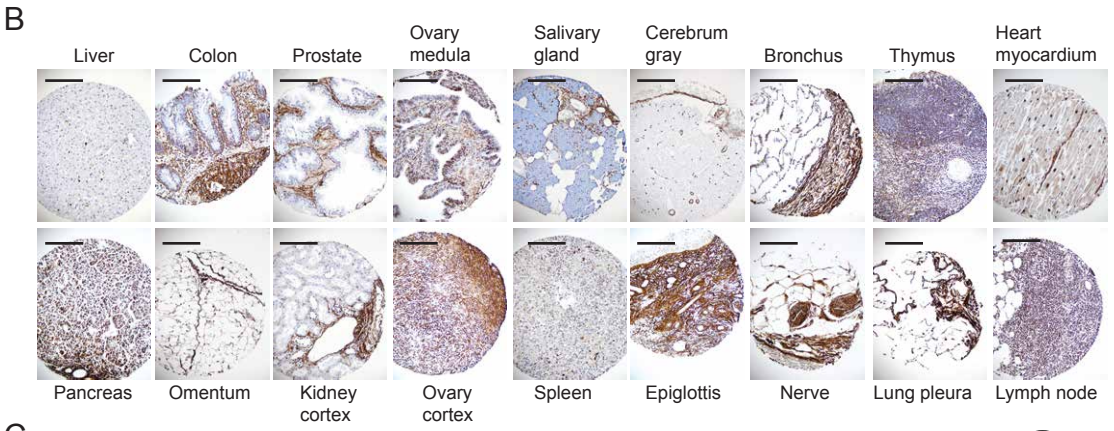

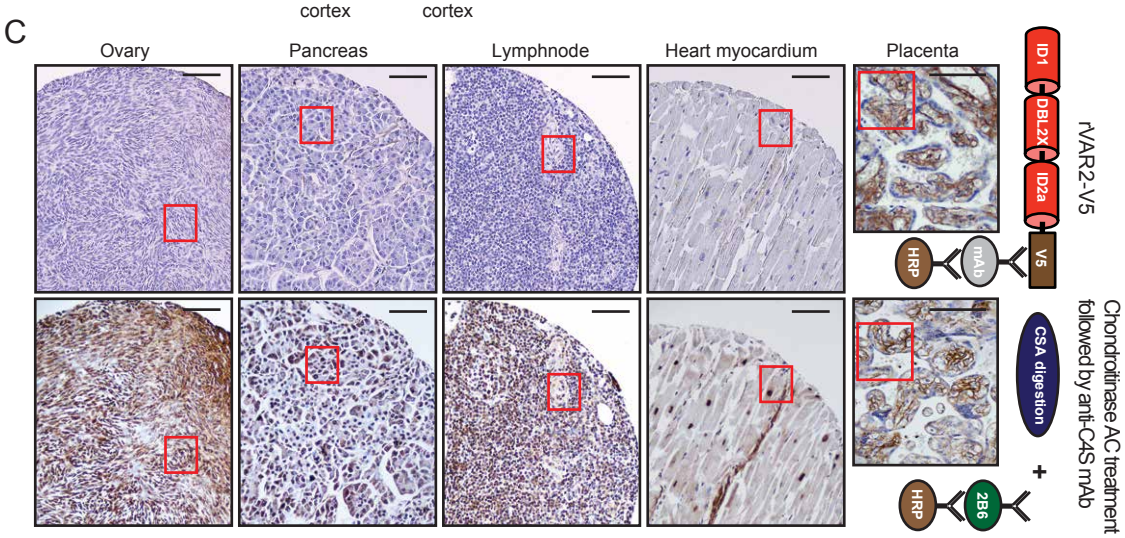

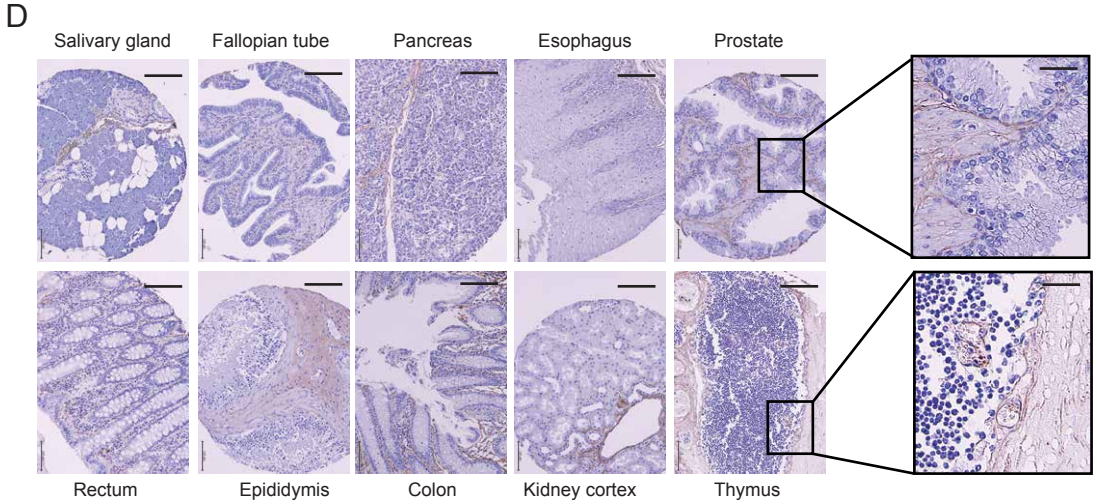

Figure S1, related to Figure 1

(**A**) 4x (left - scale bar 1 mm) and 40x (right - scale bar 150 µm) magnified images of murine placenta incubated with 500 picomolar rVAR2 and 1:700 anti-V5-HRP. Red box represents magnifications of the indicated area.
(**B**) Representative 10x (scale bar 300 µm) magnified images of indicated normal tissue cores incubated with 1 U/ml Chondroitinase AC followed by 1:20 dilution of anti-C4S (2B6) antibody.
(**C**) Representative images of indicated normal tissue specimens stained with 500 picomolar recombinant VAR2CSA and 1:700 anti-V5-HRP (upper panel) or as describe in **C** (lower panel) (Scale bar 200 µm). Red boxes represents areas presented in **Figure 1E**.
(**D**) Representative 10x (Scale bar 250 µm) magnified images of indicated normal tissue specimens incubated with 500 picomolar rVAR2 and 1:700 anti-V5-HRP. Black boxes represent magnifications of the indicated areas (Scale bar 100 µm).

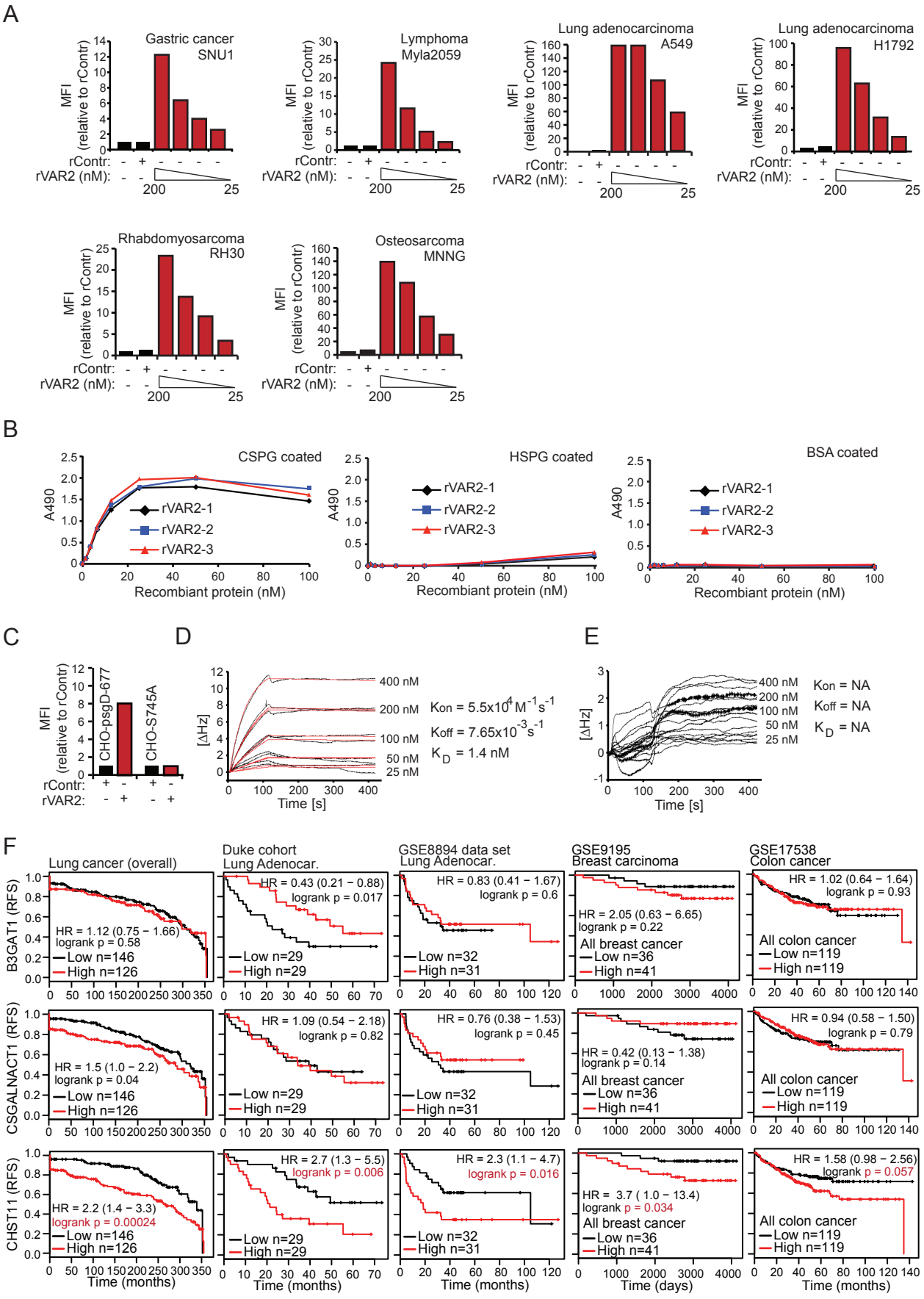
A
Gastric cancer
SNU1
Lymphoma
Myla2059
Lung adenocarcinoma
A549
Lung adenocarcinoma
H1792
Rhabdomyosarcoma
RH30
Osteosarcoma
MNNG
MFI (relative to rContr)
rContr:
rVAR2 (nM):
200
25
B
CSPG coated
HSPG coated
BSA coated
A490
rVAR2-1
rVAR2-2
rVAR2-3
Recombiant protein (nM)
C
CHO-psgD-677
CHO-S745A
rVAR2:
D
[ΔHz]
400 nM
200 nM
100 nM
50 nM
25 nM
Kon = 5.5x10^4 M^-1s^-1
Koff = 7.65x10^-3s^-1
K_D = 1.4 nM
Time [s]
E
Kon = NA
Koff = NA
K_D = NA
F
Lung cancer (overall)
Duke cohort
Lung Adenocar.
GSE8894 data set
Lung Adenocar.
GSE9195
Breast carcinoma
GSE17538
Colon cancer
B3GAT1 (RFS)
CSGALNACT1 (RFS)
CHST11 (RFS)
HR = 1.12 (0.75 − 1.66)
logrank p = 0.58
Low n=146
High n=126
HR = 0.43 (0.21 − 0.88)
logrank p = 0.017
Low n=29
High n=29
HR = 0.83 (0.41 − 1.67)
logrank p = 0.6
Low n=32
High n=31
HR = 2.05 (0.63 − 6.65)
logrank p = 0.22
All breast cancer
Low n=36
High n=41
HR = 1.02 (0.64 − 1.64)
logrank p = 0.93
All colon cancer
Low n=119
High n=119
HR = 1.5 (1.0 − 2.2)
logrank p = 0.04
HR = 1.09 (0.54 − 2.18)
logrank p = 0.82
HR = 0.76 (0.38 − 1.53)
logrank p = 0.45
HR = 0.42 (0.13 − 1.38)
logrank p = 0.14
HR = 0.94 (0.58 − 1.50)
logrank p = 0.79
HR = 2.2 (1.4 − 3.3)
logrank p = 0.00024
HR = 2.7 (1.3 − 5.5)
logrank p = 0.006
HR = 2.3 (1.1 − 4.7)
logrank p = 0.016
HR = 3.7 (1.0 − 13.4)
logrank p = 0.034
HR = 1.58 (0.98 − 2.56)
logrank p = 0.057
Time (months)
Time (days)

Figure S2, related to Figure 2

(**A**) Relative mean fluorescence intensity (MFI) of the denoted cell lines incubated with recombinant control protein (rContr) or VAR2CSA (rVAR2) as indicated and detected by flow cytometry using anti-V5-FITC.
(B) Enzyme-linked immunosorbent assay (ELISA) showing concentration dependent rVAR2 binding of three independently synthesized protein batches (rVAR2-1,2,3) to immobilized CSPG (left), HSPG (middle), and BSA (right). (**C**) Relative mean fluorescence intensity (MFI) of Immortalized CHO-psgD-677 and CHO-S745A cells incubated with recombinant control protein (rContr) or VAR2CSA (rVAR2) as indicated and detected by flow cytometry using anti-V5-FITC.
(**D-E**) Sensorgram showing binding between recombinant VAR2CSA and immobilized CHO-psgD-677 (D) and CHO-S745A (E) cells measured in delta Hertz [ΔHz] as a function of time (in seconds) using the indicated concentrations of recombinant protein. Black lines represent data, and red lines represent fitted curves attained by a 1:1 binding model. Black box summarizes K_{on}, K_{off}, and the calculated K_D value.
(F) Kaplan-Meier plots of the expression of key CS enzymes CHST11, B3GAT1 and CSGALNACT1 linked to overall survival or recurrence free survival (RFS) in indicated datasets of overall lung cancer, the Duke and GSE8894 cohort of lung adenocarcinoma, the GSE9195 breast cancer cohort and the GSE17538 colon cancer cohort. High and low expression was defined as using the median value of the selected gene as separation point. Hazard ratio (HR) was calculated using Cox proportional hazards regression, and p value was calculated using the logrank test.

Table S1, Related to Figure 2 [1]

Cancer of epithelial lineage		
A549	Lung adenocarcinoma	++
H1792	Lung adenocarcinoma	+++
BeWo	Placenta choriocarcinoma	++
C32	Melanoma	++
LCC6	Melanoma	++
Colo 205	Colorectal adenocarcinoma	+++
ES-2	Ovarian clear cell carcinoma	++
LNCap	Prostate adenocarcinoma	++
PC-3	Prostate adenocarcinoma	+++
MDA-MB-231	Breast adenocarcinoma	++
T47D	Breast ductal carcinoma	+
SNU-1	Gastric carcinoma	++
T24	Bladder transitional cell carcinoma	++
UM-UC-6	Bladder transitional cell carcinoma	+++
Cancer of mesenchymal lineage		
CW9019	Rhabdomyosarcoma	+
RH30	Rhabdomyosarcoma	++
MG63	Osteosarcoma	++
MNNG	Osteosarcoma	+++

U2os	Osteosarcoma	++
TC32	Ewing sarcoma	+
TC71	Ewing sarcoma	++
Cancer of hematopoietic lineage		
FARAGE	Diffuse Large B-cell lymphoma	0
SU-DHL-8	Diffuse Large B-cell lymphoma	+
KG-1	Acute Myelogenous Leukemia	+++
MOLP-2	Multiple Myeloma	++
MyLa 2059	Cutaneous T cell lymphoma	++
NALM-6	B cell precursor acute lymphoblastic leukemia	++
NU-DHL-1	B cell lymhphoma	++

[1] Patient-derived cancer cell lines bound by rVAR2 sorted according to cancer type. 0: no binding; +: low binding; ++: medium binding; +++: high binding. In total, 111 cancer cell lines were tested in flow cytometry of which 106 (95%) cells were positive for VAR2 binding.

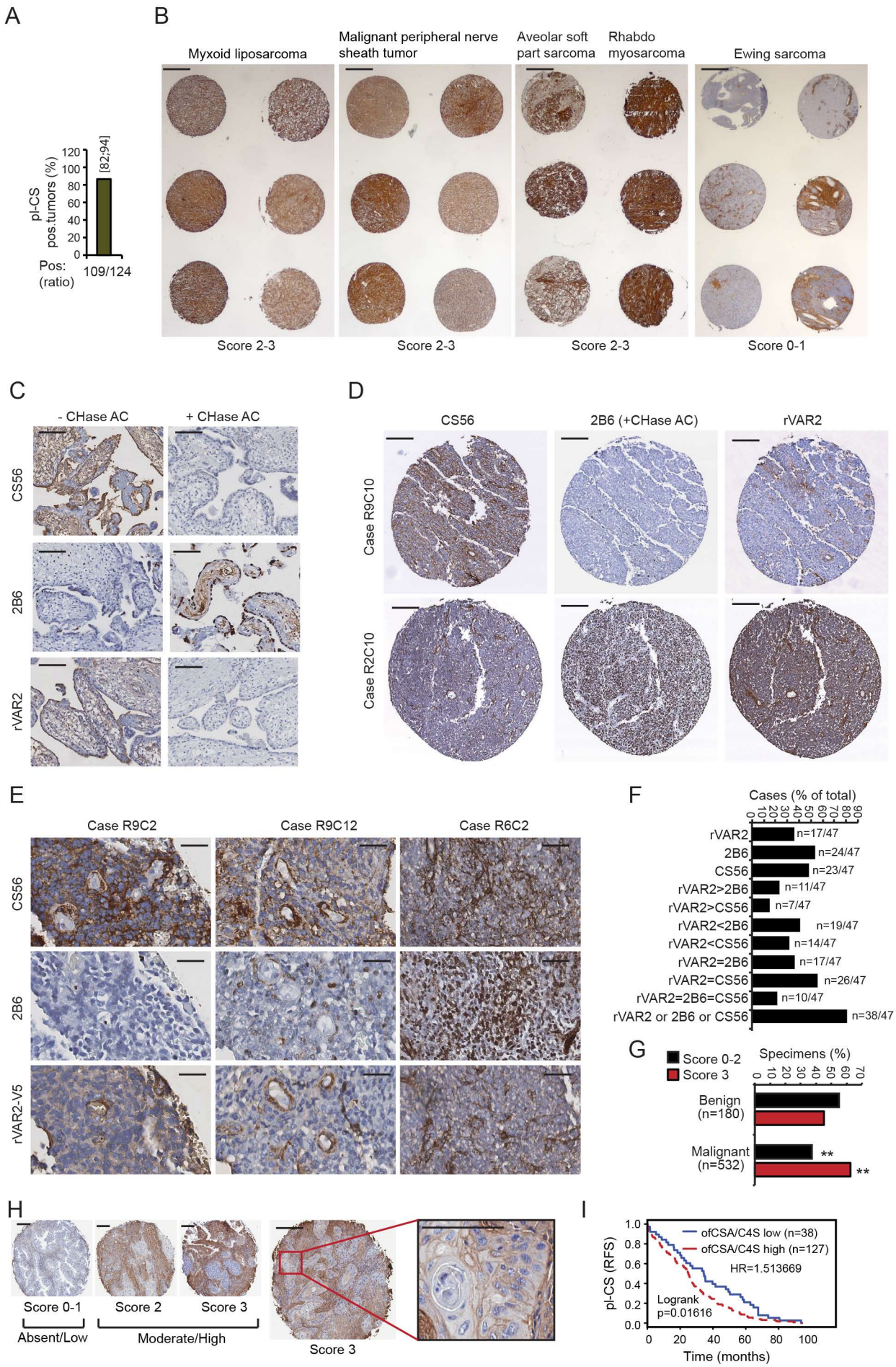
A
pl-CS pos.tumors (%)
120
100
80
60
40
20
0
[82;94]
Pos: (ratio)
109/124
B
Myxoid liposarcoma
Malignant peripheral nerve sheath tumor
Aveolar soft part sarcoma
Rhabdo myosarcoma
Ewing sarcoma
Score 2-3
Score 2-3
Score 2-3
Score 0-1
C
- CHase AC
+ CHase AC
CS56
2B6
rVAR2
D
CS56
2B6 (+CHase AC)
rVAR2
Case R9C10
Case R2C10
E
Case R9C2
Case R9C12
Case R6C2
CS56
2B6
rVAR2-V5
F
Cases (% of total)
0 10 20 30 40 50 60 70 80 90
rVAR2 n=17/47
2B6 n=24/47
CS56 n=23/47
rVAR2>2B6 n=11/47
rVAR2>CS56 n=7/47
rVAR2<2B6 n=19/47
rVAR2<CS56 n=14/47
rVAR2=2B6 n=17/47
rVAR2=CS56 n=26/47
rVAR2=2B6=CS56 n=10/47
rVAR2 or 2B6 or CS56 n=38/47
G
Score 0-2
Score 3
Specimens (%)
0 10 20 30 40 50 60 70
Benign (n=180)
Malignant (n=532)
**
**
H
Score 0-1
Score 2
Score 3
Absent/Low
Moderate/High
Score 3
I
pl-CS (RFS)
1.0
0.8
0.6
0.4
0.2
0.0
ofCSA/C4S low (n=38)
ofCSA/C4S high (n=127)
HR=1.513669
Logrank p=0.01616
0 20 40 60 80 100
Time (months)

Figure S3, related to Figure 3

(**A**) Column graph representation of placental-like CS (pl-CS) staining intensity of mixed breast cancer subtypes (n=124) scored (0-3) for binding to recombinant VAR2CSA. Column shows percentage and exact binomial 95% confidence interval of placental-like CS positive (score 2-3) tumors.
(**B**) Representative 2x (Scale bar 500 μm) magnified overview images of the soft tissue mesenchymal tumor tissue microarray (Fig. 3G) incubated with recombinant VAR2CSA (rVAR2-V5) and anti-V5-HRP and scored on a 0-3 scale for plasma membrane staining intensity where score 2 equals that of placenta.
(**C**) Representative images of human placenta specimens stained for CS expression with CS56 antibody, 2B6 antibody, and rVAR2 protein (Scale bar 100 μm). When indicated, specimens were pre-treated with chondroitinase AC to depolymerize the C4S and C6S chains down to 1 single CS unit (stub), which if C4S creates an epitope for the 2B6 antibody while removing binding of the CS56 and rVAR2 (control for binding specificity to CS).
(**D**) Representative images (4x magnification - scale bar 125 μm) of 2 (out of 47) tissue micro arrayed cases of mixed adulthood and pediatric Ewing's sarcoma treated and stained as in **C**.
(**E**) Three cases of Ewing sarcoma tissue specimens stained with CS56, 2B6 or rVAR2 as in **C** (Scale bar 150 μm).
(**F**) Ewing's sarcoma TMA (n=47) stained with the 3 reagents (CS56, 2B6, and rVAR2) where analyzed for relative staining intensity as follows **i**) rVAR2 (score 2-3) vs. 2B6 (score 0-1) (rVAR2>2B6); **ii**) rVAR2 (score 2-3) vs. CS56 (score 0-1) (rVAR2>CS56); **iii**) rVAR2 (score 0-1) vs. 2B6 (score 2-3) (rVAR2<2B6); **iv**) rVAR2 (score 0-1) vs. CS56 (score 2-3) (rVAR2<CS56); **v**) rVAR2 and 2B6 same score (rVAR2=2B6); **vi**) rVAR2 and CS56 same score (rVAR2=CS56); rVAR2 and 2B6 and CS56 same score (rVAR2=2B6=CS56); **vii**) at least one of the reagents with a score 2-3 (rVAR2 or 2B6 or CS56).
(**G**) Column graph representation of the distribution in staining intensity between benign vs. malignant soft-tissue lesions. **:p<0.0001.
(**H**) Representative images of a (n=165) non-small cell lung cancer TMA stained with recombinant VAR2CSA (rVAR2). Red box marks the amplified area of a score 3 squamous cell carcinoma. (Scale bar 250 μm).
(**I**) Kaplan-Meier plot of non-small cell lung tumor TMA stained for placental-like CSA showing recurrence free survival (RFS) of patients with low (score 0-1, n=38) or high (score 2-3, n=127) expressing tumors. Hazard ratio (HR) was calculated using Cox proportional hazards regression, and p value was calculated using the logrank test.

Table S2, related to Figure 3

Melanoma	Score 0	Score 1	Score 2	Score 3
Benign	14/49 (28.6%)	17/49 (34.7%)	17/49 (34.7%)	1/49 (2.0%)
Clark 1	0/7 (0.0%)	1/7 (14.3%)	2/7 (28.6%)	4/7 (57.1%)
Clark 2	5/32 (15.7%)	10/32 (31.3%)	8/32 (25.0%)	9/32 (28.1%)
Clark 3	2/24 (8.3%)	6/24 (25.0%)	12/24 (50.0%)	4/24 (16.7%)
Clark 4	3/23 (13.0%)	6/23 (26.1%)	8/23 (34.8%)	6/23 (26.1%)
Clark 5	0/3 (0.0%)	1/3 (33.3%)	0/3 (0.0%)	2/3 (66.7%)
Recurrent/ Metastatic	3/21 (14.3%)	1/21 (4.8%)	8/21 (38.1%)	9/21 (42.9%)

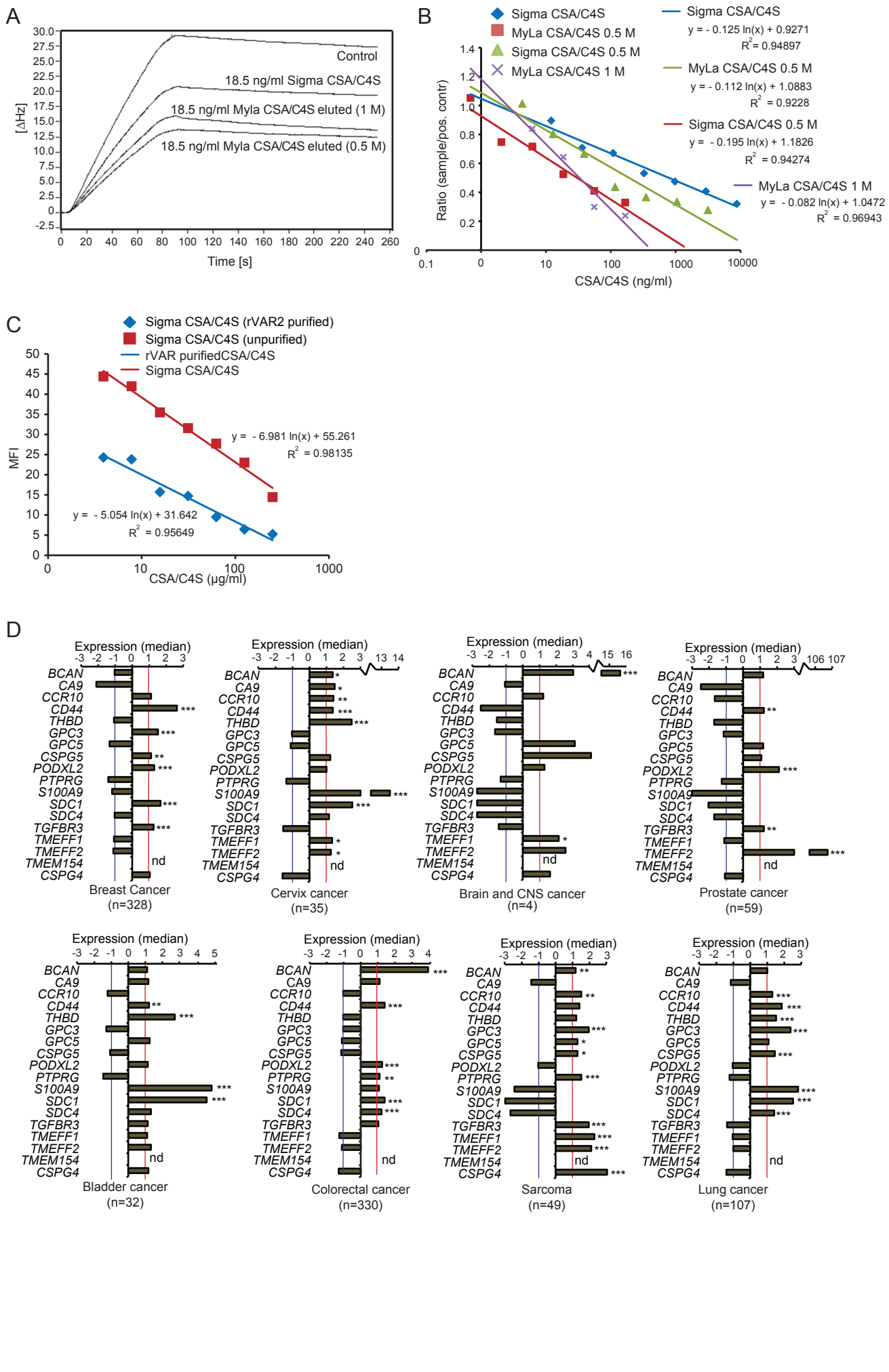
A
Control
18.5 ng/ml Sigma CSA/C4S
18.5 ng/ml Myla CSA/C4S eluted (1 M)
18.5 ng/ml Myla CSA/C4S eluted (0.5 M)
[ΔHz]
Time [s]
B
Sigma CSA/C4S
MyLa CSA/C4S 0.5 M
Sigma CSA/C4S 0.5 M
MyLa CSA/C4S 1 M
Sigma CSA/C4S
y = - 0.125 ln(x) + 0.9271
R2 = 0.94897
MyLa CSA/C4S 0.5 M
y = - 0.112 ln(x) + 1.0883
R2 = 0.9228
Sigma CSA/C4S 0.5 M
y = - 0.195 ln(x) + 1.1826
R2 = 0.94274
MyLa CSA/C4S 1 M
y = - 0.082 ln(x) + 1.0472
R2 = 0.96943
Ratio (sample/pos. contr)
CSA/C4S (ng/ml)
C
Sigma CSA/C4S (rVAR2 purified)
Sigma CSA/C4S (unpurified)
rVAR purifiedCSA/C4S
Sigma CSA/C4S
y = - 6.981 ln(x) + 55.261
R2 = 0.98135
y = - 5.054 ln(x) + 31.642
R2 = 0.95649
MFI
CSA/C4S (µg/ml)
D
Expression (median)
BCAN
CA9
CCR10
CD44
THBD
GPC3
GPC5
CSPG5
PODXL2
PTPRG
S100A9
SDC1
SDC4
TGFBR3
TMEFF1
TMEFF2
TMEM154
CSPG4
nd
Breast Cancer
(n=328)
Cervix cancer
(n=35)
Brain and CNS cancer
(n=4)
Prostate cancer
(n=59)
Bladder cancer
(n=32)
Colorectal cancer
(n=330)
Sarcoma
(n=49)
Lung cancer
(n=107)

Figure S4, related to Figure 4

(**A**) Representative sensorgram from the binding analysis (IC_{50} values) of high- and low affinity rVAR2-bound CS purified from crude bulk trachea CSA (Sigma) and from MyLa 2059 T-cell Lymphoma cells. Binding of 30 nM rVAR2 pre-incubated with the indicated CS concentrations is measured as delta Hertz [ΔHz] as a function of time (seconds). Inhibitory capacity was assessed as a decrease in peak response levels compared to the positive control.

(**B-C**) IC_{50} values were calculated from the biosensor (**B**) and FACS (**C**) analysis using linear regression. Concentration of CS is plotted against rVAR2 binding given as a ratio to the nearest positive control (B) or MFI (C). Linear regression was performed in Excel. The equations and corresponding R2 values are given in the plots, while the resulting IC_{50} values are shown in table S4.

(D) Expression of the indicated genes encoding VAR2CSA plasma membrane binding placental-like CS-modified proteoglycans Figure 4H in the indicated patient specimens extracted from the Oncomine Bitner array and divided into cancer groups. Blue and red lines represent median cut-off for average expression across the entire dataset. *p<0.05, **p<0.01, ***p<0.001. nd: not determined (missing probe).

Table S3, related to Figure 4 [1]

	Myla2059		KG-1	
Composition	Input	rVAR2 purified	Input	rVAR2 purified
Non-sulfated	1.9±1.4%	0%	2.1±1.5%	0%
Mono-sulfated	98.1±1.4%	100%	98.1±1.4%	100%
C4S	93.9%	95.8%	95.1%	95.5%
C6S	6.1%	4.2%	4.9%	4.5%
Di-sulfated	0%	0%	0%	0%

[1] Compositional analysis of extracted CS species before and after rVAR2 affinity purification. Table shows degree of sulfation as determined by LC-MS and ratio of C4S versus C6S as determined by tandem MS. Selected data is summarized graphically in Fig 5B-E.

Table S4, related to Figure 4 [1]

	Sigma CSA/C4S	Sigma CSA/C4S	MyLa2059 CSA/C4S	Placenta CSA/C4S
Affinity	Input	rVAR2 purified	rVAR2 purified	rVAR2 purified
IC_{50} µg/ml (Biosensor)	0.79	0.19	0.033	0.063
IC_{50} µg/ml (Cancer cell flow cytometry)	99.6	14.7	n.d.	n.d.
Composition				
Non-sulfated	10.5±0.5%	1.4±1.1%	0%	
Mono-sulfated	89.5±0.5%	98.6±1.1%	100%	
C4S	79.6%	90.3%	95.8%	
C6S	20.4%	9.7%	4.2%	
Di-sulfated	0%	0%	0%	

[1] Summary of the analysis of the capacity of BT-CSA, before and after rVAR2 affinity purification, and rVAR2 affinity purified Myla2059 CS and placental CS, to inhibit rVAR2 binding to immobilized CSPG in the Attana biosensor and binding to cancer cells in FACS. The composition of the different sources of CS (as in table S2) is listed below. N.d. means that experiment could not be performed due to insufficient amounts of material. Binding inhibition is shown as the concentration needed to block 50% of the binding (IC_{50} values) between rVAR2 and the cells measured by biosensor. Data is summarized in Fig 5F-G.

Table S5, related to Figure 4[1].

Gene symbol	Protein	Presence of CSA chain(s)	Known function in Cancer
BCAN	Brevican	Yes	Cell adhesion and motility. Isoforms highly expressed on cell surface in glioma (Theocharis et al., 2010)
CA9	Carbonic anhydrase IX	Proteoglycan but not previously shown to be CSA conjugated.	Involved in cell proliferation and transformation, and solid tumor acidification. Expressed in all clear-cell renal cell carcinoma, but is not detected in normal kidney (Takacova et al., 2013). Also expressed in various other tumours including breast cancers.
CCR10	Chemokine receptor 10	Not known	Chemokine receptor. Overexpressed in lymphoma, cutaneous squamous cell carcinoma (Kai et al., 2011) and melanoma. Suggested to be involved in metastasis (Murakami et al., 2004).
CD44	CD44 molecule	Yes on splicevariants	Cell adhesion and migration. Associated with a wide range of cancers and cancer stem cells (Naor et al., 1997)
THBD	Thrombomodulin	Yes	Binds thrombin. Differently expressed in a wide range of cancers including carcinoma, adenocarcinoma and glioma. Loss of TM expression correlates with certain cancer progressions. Progression of cancer correlates with serum levels of TM and high expression promotes angiogenesis and

			metastasis (Hanly et al., 2005).
GPC3	Glypican 3	HS proteoglycan but not previously shown to present CSA	Binds ECM proteins and growth factors. Has been described as an oncofetal antigen in hepatocellular carcinoma (Iozzo and Sanderson, 2011).
GPC5	Glypican 5	Yes	Binds ECM proteins and growth factors. Overexpressed in several tumors. Has been demonstrated to increase tumour proliferation in rhabdomyosarcomas by potentiating the action of FGF-2, HGF and Wnt1A (Williamson et al., 2007).
CSPG5	Neuroglycan	Yes	ND
PODXL2	Podocalyxin-like 2	Yes	Cell adhesion. Overexpressed in several tumors including breast and prostate cancer, malignant brain tumours, testicular, hepatocellular and renal cell carcinoma Overexpression has been shown to be an independent predictor of prognosis in breast, renal and colorectal cancers (Larsson et al., 2011).
PTPRG	Protein tyrosin phosphatase, receptor type, G	Proteoglycan with CS acceptor site	Enzyme involved in cell growth, differentiation, mitotic cycle, and transformation by oncogenes. Gene methylation and protein activity is associated with tumor suppression (Della Peruta et al., 2010).

S100A9	S100 calcium binding protein A9	No	A calcium- and zinc-binding protein important in the regulation of inflammatory processes and immune response. Upregulated in various cancers including hepatocellular carcinoma (HCC) (Wu et al., 2013).
SDC1 **&** ***SDC4***	Syndecan 1 & Syndecan 4	Yes	Regulates cell proliferation, differentiation, adhesion and migration. In particular Syndecan-4 is a focal adhesion component in a range of cell types and mediates breast cancer cell adhesion and spreading. Overexpressed in many cancers including prostate and breast and is key to spread of cancer. Expression correlations with tumor recurrence and poor prognosis (Theocharis et al., 2010).
TGFBR3	Transforming growth factor, beta receptor III. Also called Betaglycan	Yes (Part time)	Binds TGF. Plays a role in multiple cancers. Has been shown to decrease cancer cell motility (Mythreye and Blobe, 2009).
TMEFF1/TENB1	Transmembrane protein with EGF-like and two follistin-like domain 1 also called Tomoregulin-1	Proteoglycan with unknown modification but has several putative CS acceptor sites	Associated with prostate cancer as well as gastric cancer (Uchida et al., 1999).
TMEFF2/TENB2	Transmembrane protein with EGF-like and two follistin-like domain 1 Tomoregulin-2	Yes	Diagnostic marker for prostate cancer (Zhao et al., 2008).
TMEM154	Transmembrane protein 154	Not known but has	ND

		putative CS acceptor site	

[1]VAR2SCA plasma membrane binding-proteins identified by a functional gain-of-binding Retrogenix
screen. ND: No data available.

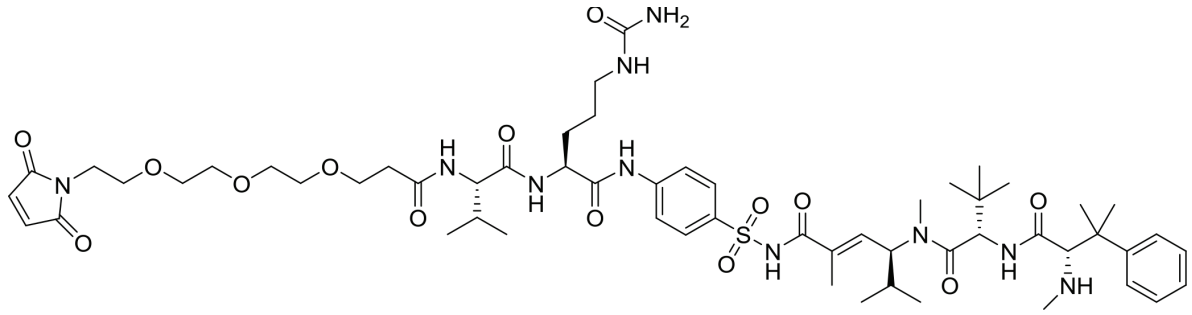

Figure S5, related to Figure 7
Structure of the protease cleavable linker-molecule MTvc886 used to conjugate KT886 to rVAR2.

SUPPLEMENTAL EXPERIMENTAL PROCEDURES

Cell lines

Human Cancer cell lines BxPC-3‡, NCI-N87‡, HCC1954‡, HCT-15‡, Capan-2‡, AsPC-1‡, Jurkat‡, MiaPaCa-2‡, OVCAR-3‡, Karpas299†, H1975◦, NCI-H358‡, SK-BR-3‡, MCF-7‡, DLD-1‡, NCI-H1437◦, HPAF-II‡, Colo205◦, MG63◦, PC-3‡, T47D‡, MDA-MB-231‡, MDA-MB-468‡, A549‡, 253J B-V◦, UM-UC-3‡, K562*, Rh30◦, U2OS◦ ,U138MG‡, A172‡, MNNG/HOS◦, JIMT-1◦, OE19†, DU145‡, HepG2‡, SKOV-3‡, KG1a‡, H292‡, and HCC1806‡ were obtained from ATCC‡, Sigma-Aldrich†, the University of Copenhagen*, or the Vancouver Prostate Centre/British Columbia Cancer Agency◦ and were cultured as instructed by the supplier. The Myla2059 Lymphoma cell lines were graciously donated by Niels Ødum at the University of Copenhagen. FARAGE, SU-DHL-8, KG-1 and NALM-6 were a kind gift from Karen Dybkaer, Aalborg University Hospital, Denmark.

Enzyme-linked immunosorbent assay (ELISA)

Plastic wells were coated with either Chondroitin Sulfate Proteoglycan (CSPG), Heparan Sulfate Proteoglycan (HSPG), or Bovine Serum Albumine (BSA) as indicated and binding of rVAR2 were detected using anti-his HRP antibody.

Immunohistochemistry

Normal tissue and clinico-pathological diagnosed tumor specimens from human patients were obtained from Origen and from tissue microarrays containing a wide variety of mesenchymal tumors (Pacheco and Nielsen, 2012). Lung cancer and melanoma samples

were obtained from patients who underwent total tumor resection. Specimen blocks chosen for the TMA met the criteria of nonnecrotic, nonirradiated, or chemo-treated lung cancer tissue. The TMA contains 231 NSCLC specimens (127 adenocarcinoma and 104 squamous cell carcinoma) and 159 mixed staged melanoma specimens. Samples were double punched 0.6 um diameter using an indexed manual arrayer with an attached stereomicroscope under the direction of a certified pathologist, who also reviewed and verified the tumor content. Test for association of CSA (low or high) with RFS in the lung TMA was performed using a one-tail Mann-Whitney test, and CSA scores with melanoma progression was performed using Goodman-Kruskal-Gamma test. $p < 0.05$ was considered significant. Using the Ventana Discovery platform, sectioned paraffin-embedded tissue samples were stained with 500 picomolar V5-tagged rVAR2 without antigen retrieval followed by 1:700 monoclonal anti-V5 step, and a anti-mouse-HRP detection step. Mounted and stained specimens were subsequently scored for membranous staining intensity on a 0-3 scale. Score 0-1 represented absent/weak staining and score 2-3 positive staining, where score 2 reflects a staining intensity equal to that of placenta (included as a positive control in each staining run). Within each cancer group the percentage and exact binomial 95% confidence interval was calculated using STATA 12 software.

Retrogenix Technology

Screening for VAR2CSA binding proteins was performed using the Retrogenix Cell Microarray technology (www.retrogenix.com). Initially 3550 expression vectors, each encoding a unique human plasma membrane protein and the fluorescent ZsGreen1 protein, were pre-spotted on glass slides. Human HEK293 cells were grown over the arrays and

reverse-transfected, resulting in the over-expression of each membrane protein and ZsGreen1. Slides were then incubated with 5 µg/ml V5-tagged VAR2 DBL1-ID2a followed by an AlexaFluor647-labeled anti-V5 antibody (AbD Serotec). VAR2CSA-binding proteins were identified by fluorescence imaging (ZsGreen1 and AlexaFluor647) and ImageQuant software (GE). For validation and specificity testing, expression vectors encoding the VAR2CSA binding proteins were re-spotted on new slides, and HEK293 cells were reverse-transfected. Slides were then treated with V5-tagged rVAR2 with or without 400 µg/ml CSA or following a 30 min chondroitinase ABC (CHase; Sigma) pre-treatment, or treated with rContr or with no ligand. Interactions were analysed using the AlexaFluor647-labeled anti-V5 antibody and fluorescence imaging. After fluorescence imaging of the slides, spot and background intensities were quantified from at least 6 high power field images representing at least 2 independent experiments using ImageQuant software (GE).

Bioinformatics

The Bittner multicancer dataset is available at http://www.oncomine.org/main/index.jsp (Rhodes et al., 2004). The dataset was analyzed for median expression of identified genes encoding VAR2CSA plasma-membrane binding proteins relative to a calculated average median expression across the entire dataset. Survival and microarray analysis were performed using the R statistical environment. Affymetrix microarray datasets linked to outcome were normalized using the Robust Multichip Array (RMA) method from affy package (Gautier et al., 2004) and optimal probe sets were selected with the Jetset package (Li et al., 2011). For the Duke and the Bild lung cancer datasets, survival analysis was

performed with the overall survival time. For all the others datasets the outcome variable is the time of recurrence free survival. Survival curves were calculated using the Kaplan-Meier method. High and low expression patients were divided using the median value of the selected gene as separation point. Hazard ratio was calculated using Cox proportional hazards regression, and p value was calculated using the logrank test.

Immunoprecipitation

Membrane proteins were extracted by lysing C32 cells with EBC lysis buffer (150 mM NaCl, 50 mM Tris-HCl, 2.5 mM MgCl2, 1 mM EDTA, 1% CHAPS and a protease inhibitor cocktail (Roche). The lysate was loaded onto a Hitrap NHS HP column (GE) containing immobilized rVAR2 or DBL4 control protein. The column was washed extensively in Lyses buffer as well as lysis buffer containing 250 mM NaCl. Bound protein was eluded with 0.5 M NaCl in lysis buffer and concentrated on a vivaspin column (MWCO 10.000 kDa). Protein samples and a high-molecular weight marker (LC5699, Life Technologies) were loaded onto a NuPAGE Tris-acetate gel (Life Technologies). Proteins were subsequently transferred to a nitrocellulose overnight at 4C at 75 mA. The membranes were stained with anti-CSPG4 antibody (LHM2, Abcam) or Anti-panCD44 (2C5, RnD systems).

Mass Spectrometry

Denaturing SEC-HRMS for intact mass analysis of recombinant VAR2 and VAR2 drug conjugates was performed on a Waters Acquity H Class UPLC with PDA detection at 280 nm utilizing an Acquity UPLC BEH 200 SEC column (1.7 uM, 4.6 mm x 150 cm).

High resolution mass spectrometry detection was achieved using a MicroMass Q-TOF Premier with a scan range from 250-4900 m/z. The analysis was performed using an isocratic elution at 0.25 ml/min over 11 min with 70/30 H20/ACN with 0.1% TFA and 0.1% FA. Data collection and analysis was done with MassLynx 4.1 with spectral deconvolution using MaxEnt1.

Subcutaneous PC3 and B16 tumor model

PC-3M-Luc-C6 cells ($2x10^6$ cells) were injected subcutaneously into the right flank of $Foxn1^{nu}$ mice on day -12. The mice were divided into 3 groups with 10 mice in each, and were treated with intravenous injections of vehicle (saline), a control DT388 fusion protein (rContr-DT), or an rVAR2 DT388 fusion protein (rVAR2-) respectively, on day 0, 2 and 6 at 0.6 mg/Kg doses. Tumor growth was monitored using a caliper-measuring tool, and the 3 longest perpendicular axes in the x/y/z plane of each tumor were measured. Tumor volume was calculated according to the standard formula: volume = xy^2*0.5236 (Janik et al., 1975). Saline and rVAR2-DT treated mice were also injected with luciferine and scanned for tumor chemiluminescence using IVIS at day 3 and 13 after 1^{st} dose (saline or rVAR2-DT). Control mice were given PBS or 0.33 mg/Kg rVAR2-NIR before sacrifice, and tumors were extracted and scanned by IVIS.

Karpas299 Xenograft Study

The in vivo efficacy study was performed at the Experimental Therapeutics & Animal Resource Centre at the BC Cancer Research Centre. Female C.B-17/IcrHsd-Prkdcscid mice (Harlan Laboratories) were anesthetized using isoflurane and were then implanted subcutaneously in the back with $1x10^6$ Karpas299 human T cell lymphoma tumour cells per mouse. Tumours were established over a period of 19 days, and test animals were then grouped according to tumour volume such that each group (n=7) had an equal distribution of tumour volumes. Dimensions of established tumours were measured with calipers. Tumour volumes were calculated according to the equation (Length x $Width^2$ /2) with the length (millimeters) being the longer axis of the tumour. The mean tumour volume on treatment day was greater than 150 mm^3. Intravenous test article administration began on Day 21, and continued every two to three days (total of three injections) at the doses indicated in the figure legend. Animals were injected based on individual body weights using a 28 G needle. Dilation of the lateral tail vein was achieved by holding the animals under a heating lamp for 1-2 min. The animals were briefly restrained (approximately 1 min) and injection was delivered into the lateral tail vein. Animal health was assessed acutely using Post Injection Clinical Observation Record (PICOR) forms. Body weights and tumour volumes were measured every Monday, Wednesday, and Friday. Animals remained on study until their tumours reached 800 mm^3 in size or they otherwise required euthanasia due to achieving a humane endpoint.

4T1 syngeneic bone metastasis model

Five to 6 weeks old C57black/6 female mice were maintained under isoflurane anesthesia and (5×10^5) 4T1-luciferase cells suspended in 100 µl of PBS solution were injected into the left ventricle under ultrasound guidance using a 30 gauge needle. The location of the tip of the needle in the left ventricle was confirmed by pulsatile blood flow in the hub of the needle. Animals were monitored until 8 weeks after injection using IVIS imaging system. Metastasis sites were collected at day of sacrifice and fixed in formalin for pathology studies.

Preparation of Drug Conjugate

To a solution of DBL1-ID2a (25.7 mg; 225 nmol) in ice cold PBS, pH 7.4 (34 ml) was added MTvc-KT886 (180 µl of a 10 mM dmso stock solution). The protein solution was mixed gently and allowed to stand on ice for a period of 70 min prior to concentration to a final volume of 12 ml by passage over an Amicon Ultra Centrifugal Filter (3000 xg; ~25 mins; 4°C; 50 kDa MWCO; Millipore product UFC905096). The concentrated protein solution was next purified over Zeba Spin Desalting Columns (40 kDa MWCO; 10 ml size; Thermo Scientific product 87772) preconditioned with sterile PBS. Concentration of the recovered materials was estimated by BCA assay using DBL1-ID2a as a standard. Composition and purity of the VDC were assessed by SDS-PAGE and SEC-UPLC-Esi-MS.

In vitro Cytotoxicity Assay of VAR2-Drug Conjugates using human Cancer Cell lines

Cells were removed from their culture vessel using Gibco® Trypsin-EDTA (Invitrogen # 25300-054). Detached cells were diluted in respective growth medium (Invitrogen #: 10313-021, A10491-01, 16600-082, 12561-056, 35050-061, 11415-064) + 10% Fetal bovine serum (Corning #: 35-015-CV) to 25000 cells/mL such that 100 µl/well will dispense 2500 cells/well. Cells were seeded into black walled, flat bottomed 96-well plates (Costar # 3904). Adherent cell lines cells were incubated for one night at 37 ^{0}C in a 5% CO2 atmosphere (No CO2 for MDA-MB-231) to allow the cells to attach to the microtitre plate surface, while suspension cells were seeded immediately before use. Test compounds were diluted directly in the appropriate cell growth medium at five-times the desired final concentration. These compounds were then titrated 1:3, over eight steps. A control with no test compound present (growth medium alone) was included on each microtiter plate in sextuplicate. 25 µl/well of the prepared titrations was added in triplicate to each cell line assayed. The cells and titrations were incubated at 37 ^{0}C / 5% CO2 for five nights. After the incubation, cell viability was measured using CellTiter-Glo® (Promega #G7572) reagent by adding thirty µl of prepared CellTiter-Glo® to each assay well. The mixtures were incubated for at least twenty min in the dark prior to measuring emitted luminescence using a microplate luminometer (500 ms integration time). The collected relative luminescence units (RLU) were converted to % cytotoxicity using the RLU values measured from the growth medium alone control as follows: % Cytotoxicity = 1 - [Well RLU/average medium alone control RLU]. Data (% Cytotoxicity vs. Concentration of

ADC (log10 [nM]) were plotted and were analyzed by non-linear regression methods using GraphPad Prism software v. 5.02 to obtain EC_{50} estimates.

***In vitro* toxicity assay using DT-VAR2**

The cells were seeded and incubated 3-5 days with toxin coupled rVAR2 or control protein. 400 µg/ml CSA was used as a specificity control. Following incubation, cells were washed in PBS and stained with Methylene Blue in Methanol or WST1 (Roche). Color was dissolved in 0.2 M Sodium Citrate in 50% Ethanol and quantified by absorbance at 450 nm. IC_{50} values were calculated as concentration of toxin at 50% survival. For a description of the in vitro tox assay using VCD886 please see supplementary methods.

Tolerability Study

Female CD-1 mice (Harlan Laboratories) were injected with the test articles and doses indicated in the figure legend using the housing/restraint/injection methods indicated above. Monitoring for acute toxicity effects was facilitated using the Post Injection Clinical Observation Record (PICOR) to assess morbidity and help determine humane endpoints. A PICOR was only completed for an animal in the event that a moribund animal was observed. Mice were monitored and weighed 3 times weekly for 12 days. Dose escalation occurred following favourable assessment of acute tolerability.

SUPPLEMENTAL REFERENCES

Della Peruta, M., Martinelli, G., Moratti, E., Pintani, D., Vezzalini, M., Mafficini, A., Grafone, T., Iacobucci, I., Soverini, S., Murineddu, M., et al. (2010). Protein tyrosine phosphatase receptor type {gamma} is a functional tumor suppressor gene specifically downregulated in chronic myeloid leukemia. Cancer research 70, 8896-8906.

Gautier, L., Cope, L., Bolstad, B.M., and Irizarry, R.A. (2004). affy--analysis of Affymetrix GeneChip data at the probe level. Bioinformatics 20, 307-315.

Hanly, A.M., Hayanga, A., Winter, D.C., and Bouchier-Hayes, D.J. (2005). Thrombomodulin: tumour biology and prognostic implications. Eur J Surg Oncol 31, 217-220.

Iozzo, R.V., and Sanderson, R.D. (2011). Proteoglycans in cancer biology, tumour microenvironment and angiogenesis. J Cell Mol Med 15, 1013-1031.

Janik, P., Briand, P., and Hartmann, N.R. (1975). The effect of estrone-progesterone treatment on cell proliferation kinetics of hormone-dependent GR mouse mammary tumors. Cancer Res 35, 3698-3704.

Kai, H., Kadono, T., Kakinuma, T., Tomita, M., Ohmatsu, H., Asano, Y., Tada, Y., Sugaya, M., and Sato, S. (2011). CCR10 and CCL27 are overexpressed in cutaneous squamous cell carcinoma. Pathol Res Pract 207, 43-48.

Larsson, A., Johansson, M.E., Wangefjord, S., Gaber, A., Nodin, B., Kucharzewska, P., Welinder, C., Belting, M., Eberhard, J., Johnsson, A., et al. (2011). Overexpression of podocalyxin-like protein is an independent factor of poor prognosis in colorectal cancer. Br J Cancer 105, 666-672.

Li, Q., Birkbak, N.J., Gyorffy, B., Szallasi, Z., and Eklund, A.C. (2011). Jetset: selecting the optimal microarray probe set to represent a gene. BMC Bioinformatics 12, 474.

Murakami, T., Cardones, A.R., and Hwang, S.T. (2004). Chemokine receptors and melanoma metastasis. J Dermatol Sci 36, 71-78.

Mythreye, K., and Blobe, G.C. (2009). Proteoglycan signaling co-receptors: roles in cell adhesion, migration and invasion. Cell Signal 21, 1548-1558.

Naor, D., Sionov, R.V., and Ish-Shalom, D. (1997). CD44: structure, function, and association with the malignant process. Adv Cancer Res 71, 241-319.

Pacheco, M., and Nielsen, T.O. (2012). Histone deacetylase 1 and 2 in mesenchymal tumors. Mod Pathol 25, 222-230.

Takacova, M., Bartosova, M., Skvarkova, L., Zatovicova, M., Vidlickova, I., Csaderova, L., Barathova, M., Breza, J., Jr., Bujdak, P., Pastorek, J., et al. (2013). Carbonic anhydrase IX is a clinically significant tissue and serum biomarker associated with renal cell carcinoma. Oncol Lett 5, 191-197.

Theocharis, A.D., Skandalis, S.S., Tzanakakis, G.N., and Karamanos, N.K. (2010). Proteoglycans in health and disease: novel roles for proteoglycans in malignancy and their pharmacological targeting. FEBS J 277, 3904-3923.

Uchida, T., Wada, K., Akamatsu, T., Yonezawa, M., Noguchi, H., Mizoguchi, A., Kasuga, M., and Sakamoto, C. (1999). A novel epidermal growth factor-like molecule containing two follistatin modules stimulates tyrosine phosphorylation of erbB-4 in MKN28 gastric cancer cells. Biochem Biophys Res Commun 266, 593-602.

Williamson, D., Selfe, J., Gordon, T., Lu, Y.J., Pritchard-Jones, K., Murai, K., Jones, P., Workman, P., and Shipley, J. (2007). Role for amplification and expression of glypican-5 in rhabdomyosarcoma. Cancer research 67, 57-65.

Wu, R., Duan, L., Ye, L., Wang, H., Yang, X., Zhang, Y., Chen, X., Weng, Y., Luo, J., Tang, M., et al. (2013). S100A9 promotes the proliferation and invasion of HepG2 hepatocellular carcinoma cells via the activation of the MAPK signaling pathway. Int J Oncol 42, 1001-1010.

Zhao, X.Y., Liu, H.L., Liu, B., Willuda, J., Siemeister, G., Mahmoudi, M., and Dinter, H. (2008). Tomoregulin internalization confers selective cytotoxicity of immunotoxins on prostate cancer cells. Transl Oncol 1, 102-109.